

**Electrochemical Analysis of Mild Steel
Coated with Polystyrene Based
Nanocomposite Coatings Simulating
Uniaxial Stress and Sea Water Service
Conditions**



**By
Asad Hayat**

**School of Chemical and Materials Engineering (SCME)
National University of Sciences and Technology (NUST)**

2017

Electrochemical Analysis of Mild Steel Coated with Polystyrene Based Nanocomposite Coatings Simulating Uniaxial Stress and Sea Water Service Conditions



Name: Asad Hayat

Reg No: NUST201463838MSCME67714F

**This work is submitted as a MS thesis in partial fulfillment of the
requirement for the degree of**

(MS in Materials and Surface Engineering)

Supervisor: Dr. Muhammad Shahid

**School of Chemical and Materials Engineering (SCME)
National University of Sciences and Technology (NUST), H-12
Islamabad, Pakistan
March, 2017**

Certificate

This is to certify that work in this thesis has been carried out by **Mr. Asad Hayat** and completed under my supervision in School of Chemical and Materials Engineering, National University of Sciences and Technology, H-12, Islamabad, Pakistan.

Supervisor _____

MS- Supervisor

Dr. Muhammad Shahid

Submitted through

Prof. Dr. Mohammad Mujahid

Principal/Dean,

School of Chemical and Materials Engineering,

National University of Sciences and Technology, Islamabad

Dedication

I would like to dedicate this dissertation to my family for their support to my higher education.

Acknowledgement

I would like to acknowledge guidance and advice given by my supervisor, Dr. Muhammad Shahid for his constant persuasion, affectionate guidance and efficient supervision at each stage of this research work. I would also thank my committee members Prof. Dr. Mohammad Mujahid, Dr. Nasir Ahmad and Dr. Habib Nasir for giving valuable guidance and suggestions to improve my thesis.

Thanks to Dr. Ahmad Nawaz for his guidance during this research work. Also thanks to my seniors Mr. Abdul Saboor and Mr. Umar Faoq for sharing their valuable knowledge.

At last most importantly, the position I stand now would not have been possible without care, support and prayers of my family. They are source of ultimate encouragement for me.

Mr. Asad Hayat

Abstract

In modern science corrosion protection, has become a multidisciplinary subject. With development of new materials their anticorrosive properties in service conditions are important to study for their applications. In this work, Electrochemical analysis of Mild Steel coated with Polystyrene, Polymer blend (PANI-PS) and Nanocomposite (GNP's Reinforced polymer blend) at uniaxial stress and unstressed conditions in sea water (electrolyte) was done. Electrochemical Impedance Spectroscopy (EIS) and Tafel Scan analysis tools were used on Gamry Potentiostat whereas Scanning Electron Microscopy (SEM) was done for qualitative analysis. In EIS test, PS showed higher charge transfer resistance than Polymer blend and nanocomposite. Whereas corrosion rate determined by Tafel scan for Polymer blend and nanocomposite coatings was lower than PS coated Mild steel. SEM showed salts deposits in after corrosion tested samples without showing any crack in coatings. Corrosion behavior of stressed and unstressed samples was same. Showing that generated strain because of applied stress was not enough to degrade coating mechanically. In response to this, coatings provided excellent corrosion protection in both stressed and unstressed conditions.

Table of Contents

Dedication	I
Acknowledgement.....	II
Abstract	III
Chapter 1	1
Introduction	1
1.1 Motivation	1
1.2 Corrosion	1
1.2.1 Electrochemical Aspect of Corrosion	2
1.3 Nanocomposites	3
1.4 Polymer Blend	4
1.5 Polystyrene	8
1.6 Polyaniline (PANI)	9
1.7 Graphene Nano Particles (GNPs)	10
1.8 Dip Coating.....	15
1.9 Electrochemical Impedance Spectroscopy (EIS)	15
Chapter 2.....	17
Literature Review.....	17
Chapter 3.....	24
Experimental Work.....	24
3.1 Sample Preparation.....	24
3.2 Tensile Test	24
3.3 PANI Synthesis	24
3.4 Polystyrene Coating	25
3.5 PANI-PS Polymer Blend.....	26
3.6 GNPs Reinforced Polymer Blend.....	27
3.7 Electrochemical Analysis of Samples	27
3.7.1 Tafel Scan.....	27
3.7.2 EIS Test.....	28
3.7.3 Cell Setup.....	29
3.8 Scanning Electron Microscopy (SEM).....	31
Chapter 4.....	32

Results and Discussion.....	32
3.1 Tensile Test	32
4.2 EIS Behavior of Capacitive Coating	33
4.3 Bare Metal	34
4.3.1 EIS of MS.....	34
4.3.2 Equivalent Circuit Modelling for Bare Metal	36
4.3.3 Tafel Scan of MS	37
4.3.4 Mechanism of Steel Corrosion.....	38
4.4 Polystyrene (PS).....	39
4.4.1 EIS of PS Coated MS.....	39
4.4.2 Equivalent Circuit Modeling for Coated MS	40
4.4.3 Tafel Scan of PS Coated MS.....	42
4.4.4 SEM of PS Coated Steel	43
4.5 PANI-PS Polymer Blend Coating	44
4.5.1 EIS of Polymer Blend Coated MS	44
4.5.2 Mechanism of EIS and Circuit Modelling	45
4.5.3 Tafel Scan of PANI-PS Polymer Blend Coated MS.....	45
4.5.4 SEM of PANI- PS Polymer Blend Coated MS.....	47
4.6 GNP's Reinforced Polymer Blend (Tri-component) Coated MS	48
4.6.1 EIS of GNP's Reinforced Polymer Blend Coated MS	48
4.6.2 Mechanism of EIS and Circuit Modelling	49
4.6.3 Tafel Scan of GNP's Reinforced Polymer Blend Coated MS	49
4.6.4 SEM of GNPS's Reinforced Polymer Blend Coated MS	50
4.7 Comparative Result of EIS.....	51
4.8 Comparative Result of Tafel Scan.....	52
Conclusions.....	54
References.....	55

List of Figures

Figure 1: Corrosion Fatigue failure	2
Figure 2: Electrochemical reaction showing Zn in HCl solution.....	3
Figure 3: Composite and Nano composite comparison (a) interparticle distance (b) particle surface area.....	3
Figure 4: Different Glass Transition Behavior of Polymer Blends	6
Figure 5: Method 1; Insitu Polymerization, Method 2; Solution Processing.....	7
Figure 6: Representation of Polymer Blends	7
Figure 7: Representation of Copolymers	8
Figure 8: Polystyrene structure	8
Figure 9: Structure of Polyaniline (PANI)	9
Figure 10: Properties and Applications of PANI	10
Figure 11: Filler Geometries	11
Figure 12: Atomic structure on Graphite and Graphene.....	13
Figure 13: The number of graphene platelets and their total surface area at 1 vol% Gnp's	14
Figure 14: XRD patterns for Graphite (lower one) and GNP's (above one)	14
Figure 15: Coating Stages	15
Figure 16: Cell setup for EIS	16
Figure 17: PANI preparation method.....	25
Figure 18: Polystyrene Coating Schematic Diagram	26
Figure 19: Polymer Blend Coating Synthesis	26
Figure 20: Nanocomposite synthesis Schematic diagram.....	27
Figure 21: EIS Cell Setup	28
Figure 22: Test Setup Drawing	30
Figure 23: Cell Setup for Corrosion testing	30
Figure 24: Material Flow Chart.....	32
Figure 25: Stress-Strain graph of Mild Steel.....	33
Figure 26: Bode Plot for Capacitive Coating	33
Figure 27: Nyquist Plot for Capacitive Coating.....	34
Figure 28: Bode Graph of Bare MS	35

Figure 29: Nyquist Graph of Bare MS	35
Figure 30: Circuit Model for Bare Metal	36
Figure 31: Tafel Scan of Bare Metal.....	37
Figure 32: Pictorial Presentation of Crevice Corrosion	39
Figure 33: Bode Plot Showing EIS of PS coated MS	39
Figure 34: Nyquist Plot showing PS coated MS	40
Figure 35: Circuit Model Representing Coating.....	41
Figure 36: Tafel Scan of PS coated MS	42
Figure 37: Bode Plot Showing PANI-PS Polymer Blend Coated MS.....	44
Figure 38: Nyquist Plot Showing PANI-PS Polymer Blend Coated MS.....	45
Figure 39: Tafel Scan PANI-PS Polymer Blend Coated MS.....	46
Figure 40: Bode Result of GNP's Based Polymer Blend	48
Figure 41: Nyquist Plot for GNP's Reinforced Polymer Blend Coated Under Stress	48
Figure 42: Tafel Scan of GNP's Reinforced Polymer Blend Coated MS	49
Figure 43: Comparative Result of EIS	51
Figure 44: Comparative Result of Tafel Scan.....	52

List of Abbreviations

E_{oc}	Open Circuit Voltage
EIS	Electrochemical Impedance Spectroscopy
E_{corr}	Corrosion Potential
I_{corr}	Corrosion Current
PS	Polystyrene
PANI	Polyaniline
GNP's	Graphene Nanoparticles
R_{pore}	Pore Resistance
C_c	Coating Capacitance
R_p	Polarization Resistance
CR	Corrosion Rate
mpy	Mils per year
R_{sol}	Solution Resistance
C_{dl}	Double Layer Capacitance
SEM	Scanning Electron Microscope
SCC	Stress Corrosion Cracking

Chapter 1

Introduction

1.1 Motivation

Corrosion is an electrochemical destruction of metal because of its environment. Industrial nation is spending 5% of its income on corrosion losses which can be directly in the form of corrosion, extra material design, production loss or maintenance cost resulted because of corrosion[1].

Many corrosion protection techniques are used such as: corrosion inhibitors, anodic or cathodic protection, design modification and coatings. Coatings basically act as barrier between structural metal and environment. With the advancement in the field of material new coating materials are introduces for corrosion protection applications.

In this work, Mild Steel (M.S) tensile testing samples were coated with three types of coatings; Polystyrene (P.S), Polystyrene and Polyaniline (PANI) blend and tri system Nanocomposite of Polystyrene, Polyaniline and Graphene Nano Particles (Gnp's). Then corrosion study of these coated steel samples was done with and without uniaxial stress conditions.

1.2 Corrosion

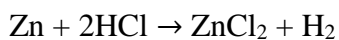
Worldwide, for structural application Mild Steel is most commonly used material. But its vulnerability to corrosion increases its maintenance cost. Though in corrosive environments on its surface a passive layer is formed but that is not strong enough as in case of stainless steel. So, for its application corrosion inhibitors, coatings, phosphating, anodic or cathodic protection is used to minimize corrosion damage[2]. In stress conditions the effect of stress combined with corrosion also increases degradation rate causing failure of material below its yield strength and design stress[3]. Corrosive environment in the presence of stress can act as pit generation site and can lead to stress corrosion cracking (SCC)[4].



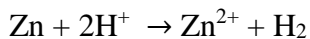
Figure 1: Corrosion Fatigue failure [5]

1.2.1 Electrochemical Aspect of Corrosion

As said earlier corrosion is an electrochemical phenomenon in which chemical reaction which is loss of metal occurs, as measure valence number of loss of electrons. Whereas gain of electrons result evaluation H_2 or Water as H_2O on the basis on environment (electrolyte). This electrochemical nature can be best understood by considering an example of Zinc (Zn) immersed in Hydrochloric acid (HCl) solution. Overall reaction of this condition can be shown as



Basing on oxidation and reduction states of elements in this reaction can be written as



From this reaction, it is evident that H^+ in solution is oxidizing Zn to Zn^+ and itself is being reduced to H_2 . Now corrosion principle for metals can be explained as **rate of oxidation and reduction reactions are always equal[6]**.

Following is pictorial explanation of this reaction:

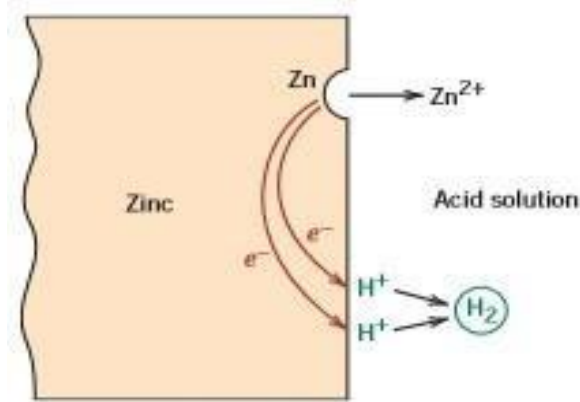


Figure 2: Electrochemical reaction showing Zn in HCl solution[1]

1.3 Nanocomposites

Polymers generally have low moduli and strength as compared with ceramics and metals. However, their mechanical properties can be improved using reinforcement[7]. This reinforcement in the form of filler can range from macro to Nanoscale increasing specific strength of polymers (now composites) from metals and ceramics. Nano level fillers provide higher particle surface area to volume fraction ratio than macro composites resulting better properties.

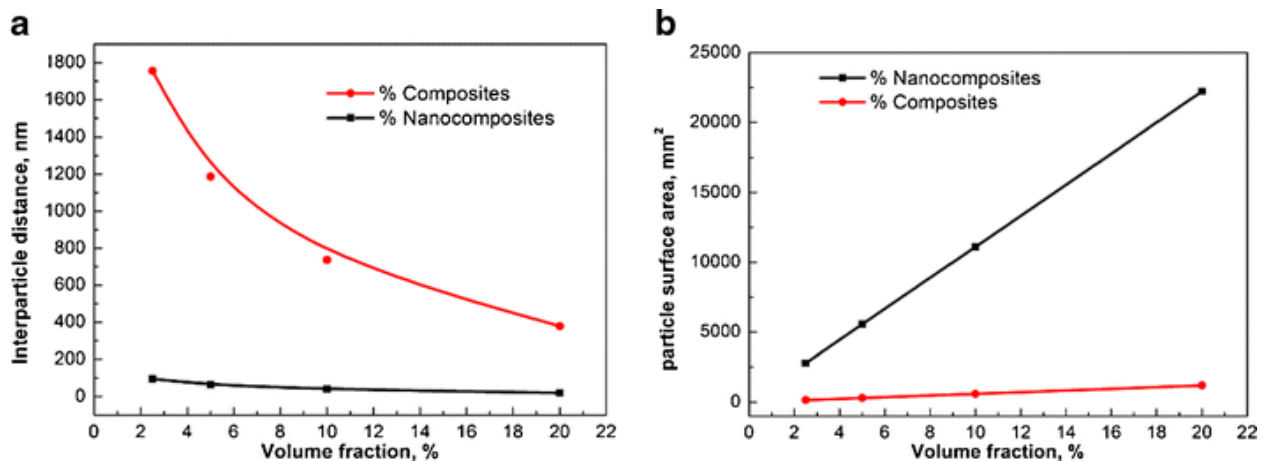


Figure 3: Composite and Nano composite comparison (a) interparticle distance (b) particle surface area[7]

Figure 3 shows that interparticle distance in case of nanocomposites is much more reduced than composites. Similarly, nanocomposites provide higher particle surface area than composites. Properties improvement in composites is directly related to area at the

interface of polymer and filler. Nano fillers in nanocomposites providing higher surface area leads this effect[8]. Polymer nanocomposites are the well-known amongst all the Nano materials, they are broadly studied for a large number of applications as flame retarding panels, high barrier films for packaging applications, anti-scratch coatings for protection of surface and high performance composites for the aerospace and automotive industry.

Unlike the materials like metals and ceramic, polymers production costs are lower and they have high specific strength, and less energy is required for the production and recycling. In the automotive industry, polymer flexibility and weight savings offered reduction in fuel consumption and a reduction of the exhaust gas as compared to the metal parts. Despite the advantages, the most important drawbacks of the polymers include a low mechanical properties and thermal stability and the lack of functionality. For example, Automotive parts, should not deform when exposed to sunlight and heat from the engine, aircraft components must be able to resist lightning and pads of brakes should be bearing the heat of friction. These require the development of polymer based composites. The combination of two materials or more than two materials has the potential to enhance the properties as compared to the neat polymer.

1.4 Polymer Blend

Polymer blend is mechanical mixture of two or more than two polymers. Polymers which don't have chemical interaction between their chain, in blend show combination of their properties. Two polymers may or may not be miscible to each other. Miscible polymers blend which are single phase show same T_g whereas immiscible polymers show more than one T_g [9]. Polystyrene and Polyaniline can be blended together using a common solvent which can dissolve both to make a solution and drying of which will give polymer blend of these two polymers[10].

In the mid-20th century the commercial emergence of new monomers, for preparing new polymers was endless. It was found that the development of new methods for the modifying the existing polymers would economically be feasible.

The first method developed for the modification was the polymerization, in other words the common polymerization of more than one species of the polymer.

The new modification process that is simple mechanical mixing of two polymers called as blending creates a new class of polymers called polymer blend.

In broad sense, any finely distributed combination of two or more polymers. In narrow sense, it can be that there should not be any chemical bonding amongst the various polymers in the blend. Combination of two or more polymer chains of constitutionally or configurationally different features, which are not having bonding with each other.

Blends of two polymers can be miscible or immiscible (mixture of two polymers remains phase separated). This is normally due to the positive heat of mixing and very little entropy of mixing. Some pairs like Polystyrene and polybutadiene, PS and PMMA etc. are immiscible polymers.

These are the commercial polymers and their blending still gives good results for example the blend of PS and Polybutadiene has increased impact strength by adding of percent polybutadiene in the PS. On the other hand, some polymer pairs like PS and poly vinyl ether, polyethylene oxide and poly acrylic acid are miscible blends. Polystyrene is also miscible with poly(2,6-dimethylphenylene), PPO. Commercial composition uses HIPS blended with PPO which increases the toughness of the system.

Glass transition temperature in case of polymer blends is an important parameter, miscible polymer blends which are single phased show the one glass transition point, whereas the immiscible polymer blends show more than one glass transition points and each polymer in blend retains its original glass transition temperature[11].

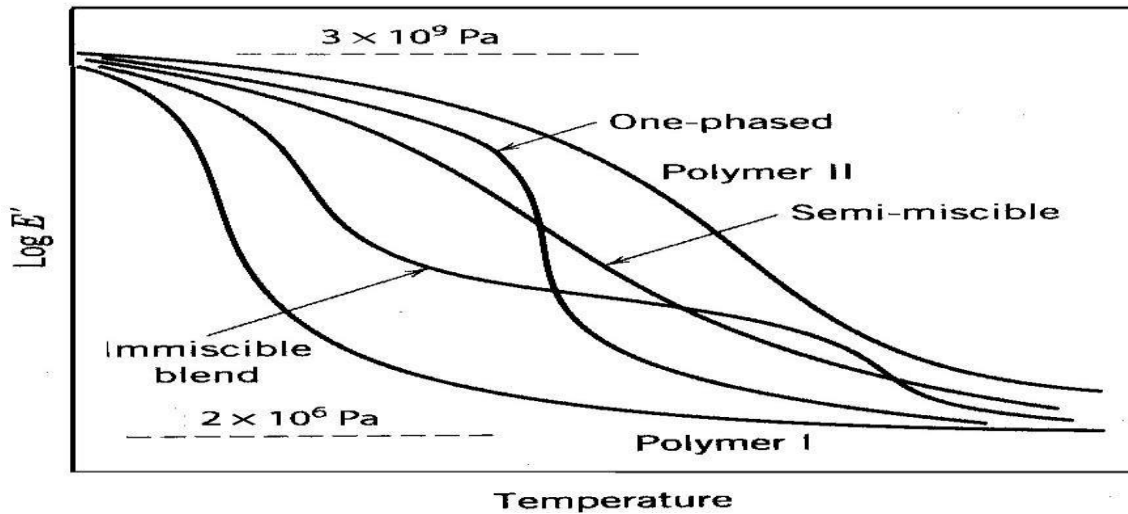


Figure 4: Different Glass Transition Behavior of Polymer Blends[11]

Polymers like polystyrene can also be blended with conducting polymers like polyaniline, so that some conducting behavior might be imparted into the polystyrene. Similarly, other polymers can also be blended with polyaniline or some other conducting polymers to achieve optimum mechanical and dielectric properties.

There are many methods to prepare polymer blends like solution processing method, in-situ polymerization, melt blending etc. Blends prepared by these methods might be showing different behaviors because of differences in the preparation methods. Some suitable solvent is required for solution processing and in-situ polymerization in which polymers are soluble. In case of melt blending no solution is required, polymers are heated above glass transition temperature then cooled to achieve some shape.

Fig 5 shows the difference between in-situ polymerization and solution blending technique for polystyrene and polyaniline blend, both techniques require some solvent, the difference is in the stage at which two different solutions are mixed together.

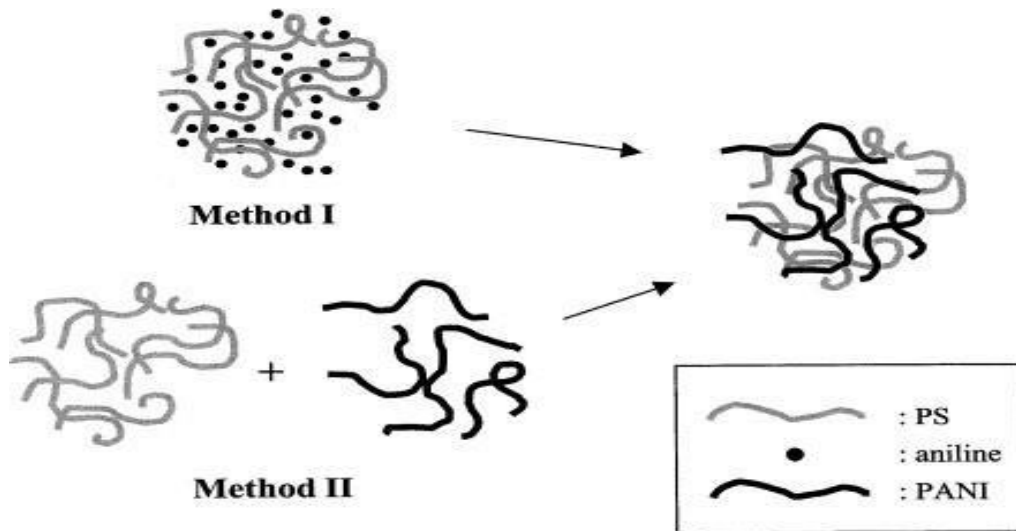


Figure 5: Method 1; In-situ Polymerization, Method 2; Solution Processing[12]

Four basic ways of combining two and more than two polymers are known (a) Polymer blend; consists a mixture or the mutual solution of two or more than two polymers, but do not have chemical bonding in between, Figure 6. (b) The graft Copolymer; constitutes a backbone of one polymer having covalently bonded side chains of another polymer. (c) A block copolymer; Figure 7 constitutes a combination of two polymers end on end by the covalent bonding clustered in separate groups. (d) A semi-interpenetrating network of polymer; comprises the entangled linking of two polymers, one of them is cross-linked, which are not bonded with each other[13].

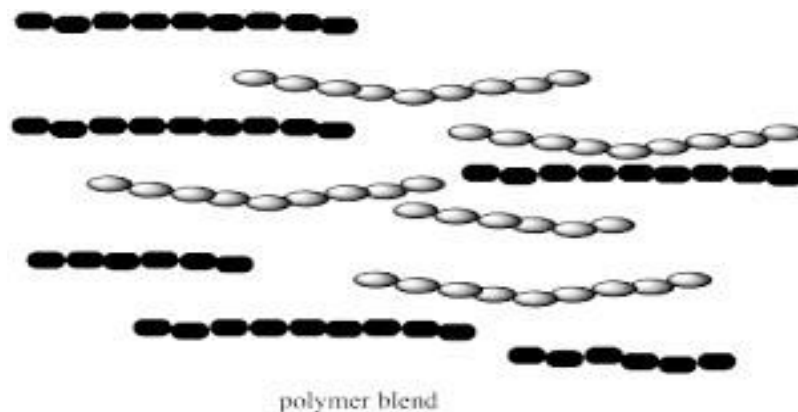


Figure 6: Representation of Polymer Blends[13]

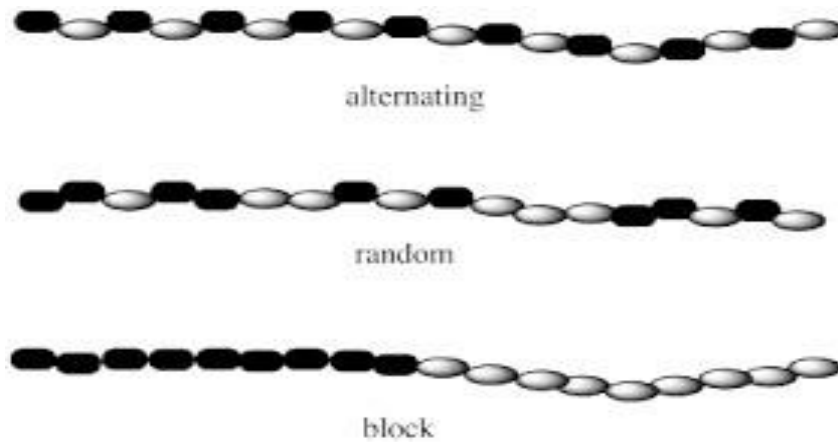


Figure 7: Representation of Copolymers[13]

1.5 Polystyrene

Polystyrene is thermoplastic polymer coming in aromatic (Benzene ring in structure) structure. Styrene monomer is polymerized to polystyrene. At ambient conditions it possess solid glassy appearance, 100°C is glass transition (T_g) temperature for polystyrene on which is it starts flowing[14].

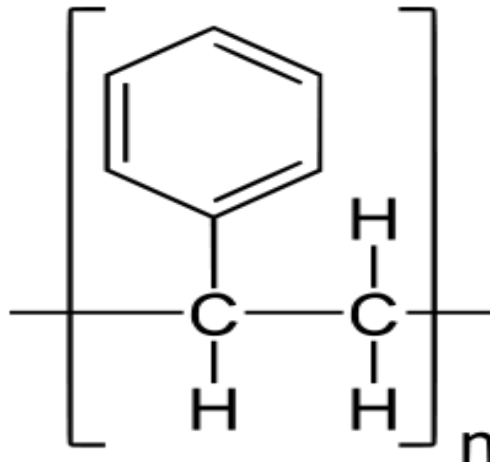


Figure 8: Polystyrene structure[14]

Polystyrene can be semi crystalline or amorphous depending on atomic arrangements in structure. Semi crystallinity comes when phenyl group is arranged at alternative sides giving syndiotactic type. Whereas, if phenyl group is randomly arranged then it gives

amorphous structure called as atactic type[15]. Amorphous polystyrene is commercially important of its types. Some physical and mechanical properties are mentioned in table below.

Table 1: Physical and Mechanical Properties

Polymer	Tg	Density g/cm ³	Tensile strength MPa	Young's Modulus MPa
Polystyrene (PS)	90 °C	1.05 at 25°C	40-60	3000- 3600

Polystyrene is transparent in nature but can be colored by adding some colorant and is used in disposable cutlery, packaging, trays, lids, containers and bottles[14].

1.6 Polyaniline (PANI)

Polyaniline is one of peculiar kind of polymers which are conductive in nature. Conductivity is because of doping conditions in its conjugated bonds. Features of conductivity, low density and easy processing makes it replaceable over metals and ceramics in applications where conductivity is most important property. Different forms of PANI have their own color, conductivity and stability[16]. Chemical structure of PANI is shown below.

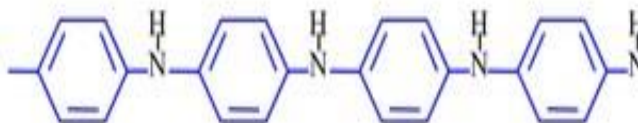


Figure 9: Structure of Polyaniline (PANI)[17]

Among properties, its glass transition temperature of PANI emeraldine was observed as 130°C. PANI has good conductivity but has very bad mechanical properties making it non ideal for practical applications[18]. Some of the properties and application are shown in figure 6:

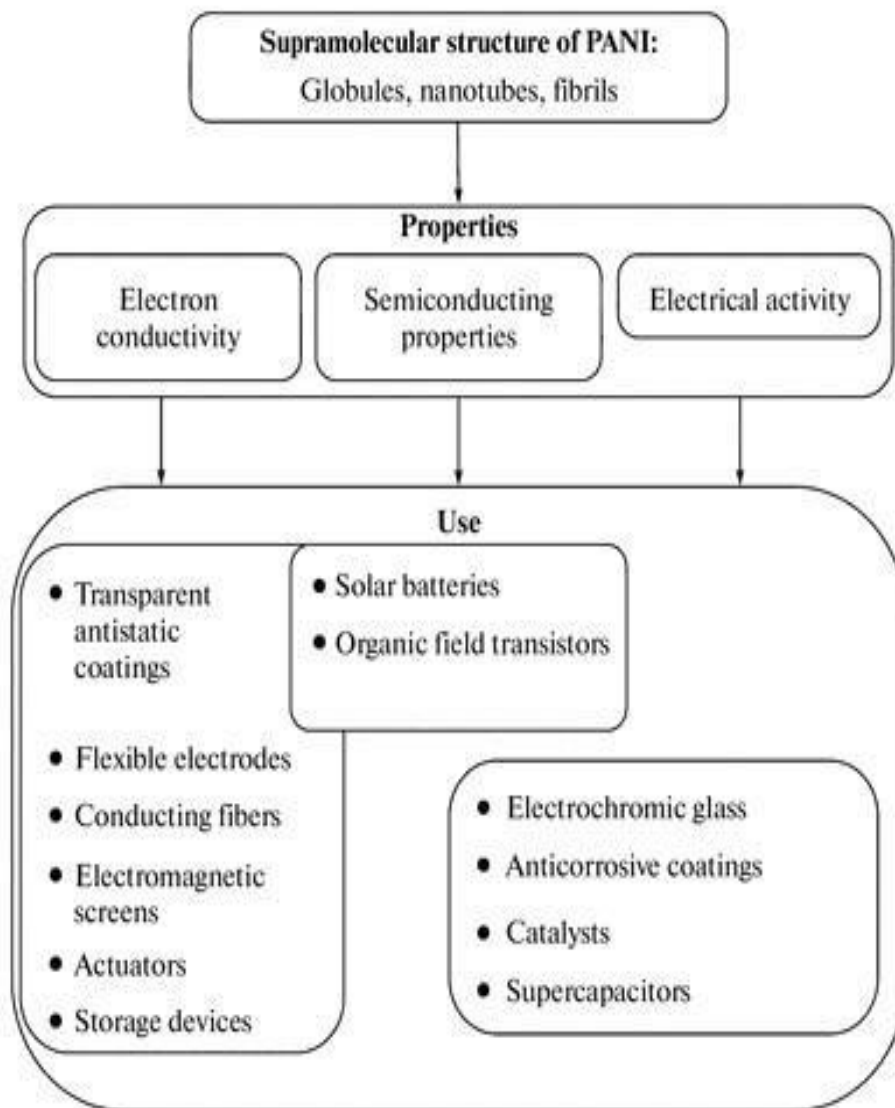


Figure 10: Properties and Applications of PANI[17]

1.7 Graphene Nano Particles (GNPs)

Fillers are used as a raw material in the production of different kind of materials and have the production of about 50 million tons each year[19]. They were used mainly for reducing the cost of the expensive binding material initially and to improve the physical characteristics of the resulting composite. Filler's purpose is changing now a day, firstly their prime function was to lower the production costs that is now changing towards the improvement of properties of materials such as tensile or compression strength,

workability, and flame retardancy. Nano fillers are the fillers which have at least one critical dimension less than 100nm. They can be in form of small spherical particles, rod shaped objects or flakes, figure 11.

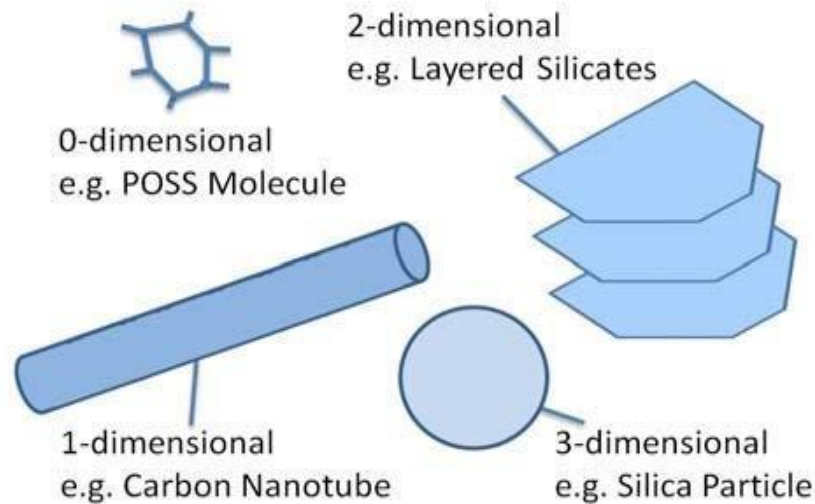


Figure 11: Filler Geometries[19]

Many Nano fillers like POSS (Polyhedral oligomeric silsesquioxane), Nano-clays, carbon Nano tubes, silica particles, graphene, graphene Nano platelets and carbon black are being used in polymer Nano composites having their specific geometries as mentioned above in figure 11.

POSS (Polyhedral oligomeric silsesquioxane) molecules are a new approach to new nanocomposite. The benefit of a molecular approach is in a real dispersion in the nanometer range. POSS molecules is used as a reinforcing filler in plastic material to increase the mechanical strength. They have also been used as abrasion resistance in paints and coating as flame retardants in polymers.

Fumed silica is usually a form of silicon dioxide in non-crystalline state. Particle sizes ranges from 5-30 nm which are transferred into larger agglomerates keeping the large specific surface area of 10 to 600 m²/g.4, fumed silica can be generally referred to as anti-klonter agent and a thickening agent with thixotropic property[20].

Nano-clays are nanoparticles having plate like structure and are natural phyllosilicates, clays can be of various types, such as bentonites and hectorites. Bentonite is majorly montmorillonite, common Nano-clay used in material applications. Montmorillonites, the stacked nanoscopic alumino silicate plates each about 1 nm high and 1 urn in diameter and are used as a filler in plastics. Montmorillonites which are organically modified, so called organo clays, are commonly used to improve the flame retardancy in polymers, particularly for cables[20].

Carbon nanotubes (CNTs) have been extensively studied because of its good mechanical and electrical properties. An important application of multi-walled carbon nanotubes (MWNT) can be that they are used as functional fillers in plastic composites and coatings. They are also used as reinforcing filler in concrete and used to avoid crack propagation[21].

Graphite is also used as a filler in paints and coatings for electrical conduction, wherein the antistatic properties is obtained. Its two-dimensional shape is graphene, that may be thought of as a single layer or sheet of graphite. Graphene can be used as a filler in conductive and reinforcement applications.

GNPs come in category of Nano fillers. Nano fillers are those which have one dimension at least less than 100nm. In past fillers were used to reduce the cost of material but now their purpose has changed. Now they are used to improve properties of material such as compressive and tensile strength and thermal property such as flame retardancy[22].

GNPs are short 5 to 8 stacks layers of graphene sheets having platelet like shape and thickness about 6 to 8nm. They have high mechanical properties also, very good electrical and thermal properties because of graphitic composition. GNPs can be used with polymers to enhance their thermal and mechanical properties.

Expanded Graphene (EG) is generated using sulfuric and nitric acid mixture to intercalate graphite and then using microwave or heating to exfoliate layers. EG has a layer structure but interlayer distance is higher than that of graphite. Now plates are 30 to 80 nm thick but have lost stacking. EG is a Nano filler but has low specific surface area. This can be increased by further exfoliation which results it to be GNPs. Thickness of GNPs depend on production method. Through sonication GNPs of 10nm thickness can be made. Another way, by sonication of graphite in water can result highly defect free single or multilayers graphene. But surfactants used in this results in decrease in electrical conductivity[23].

Figure 12 shows the atomic structure of graphite and graphene, graphene is a single layer whereas graphite contains many graphene layers. Table 2 shows the thickness of different graphene derivatives[8].

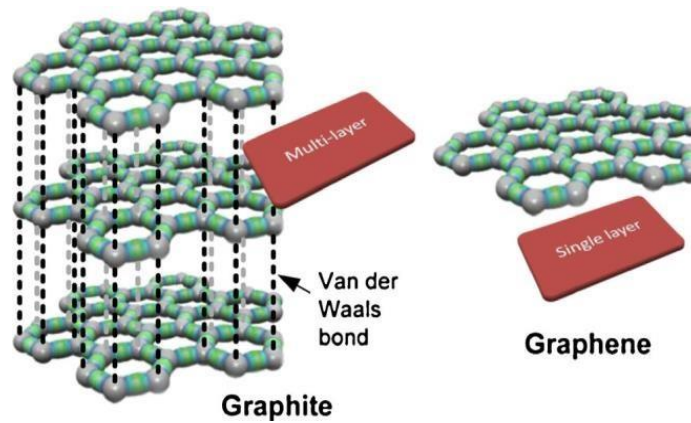


Figure 12: Atomic structure on Graphite and Graphene[8]

Table 2: Typical thickness of graphene derivatives[8]

Graphene derivatives	Thickness
Graphite	0.4-60 μm
Expanded graphite	100-400nm
Graphite nanoplateles	5-100nm
Graphene nano platelets	0.34-5nm

Figure 13 shows that as the average thickness of graphene platelets increases, the total number of platelets and the surface area of the platelets decreases. So, at low thickness values higher interaction is expected.

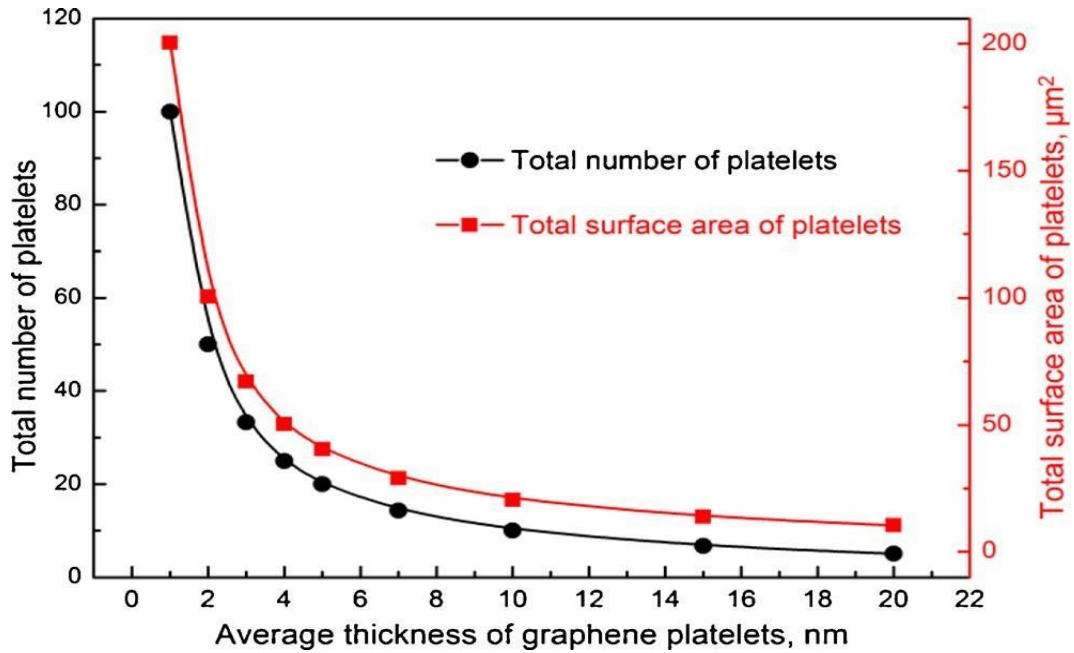


Figure 13: The number of graphene platelets and their total surface area at 1 vol% Gnp's[8]

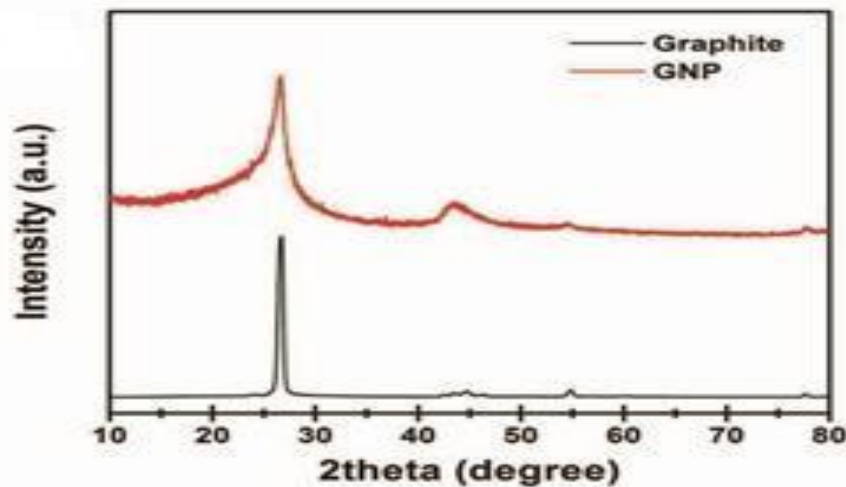


Figure 14: XRD patterns for Graphite (lower one) and GNP's (above one)[24]

In figure 14 we can see the difference between graphite and GNP as they show difference in the patterns. At 2theta 26.2-degree graphitic peak is observed in the lower pattern which is for graphite in the above pattern in fig 1.10b that graphitic peak is broadened due to decreased graphitic particle size in GNP. GNP consists of few stacked graphene layers. Diameter of GNP is few hundred nanometers[24].

1.8 Dip Coating

Dip coating is simple, inexpensive and efficient technique. It is fast and requires less equipment as compare with other techniques[25]. This technique has three steps[26].

- Immersion- Substrate (to be coated) is immersed in to coating (solution)
- Dwell Time- Time substrate remains in solution
- Evaporation- removing and drying of coating applied

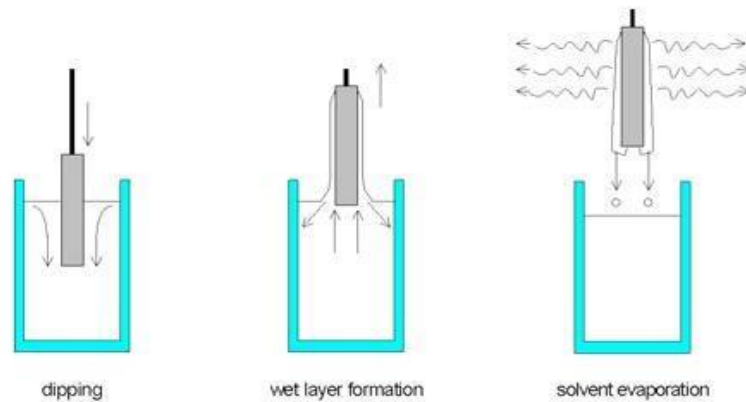


Figure 15: Coating Stages[26]

1.9 Electrochemical Impedance Spectroscopy (EIS)

EIS is useful technique of electrochemistry and can be used to evaluate electrochemical interface and coating characterization. For Electrochemical cell and AC (usually 10mV) is applied, in response to which cell shows current. Now varying applied frequency coating response can be measured[27].

For coatings study cell setup is done as shown in figure 8:

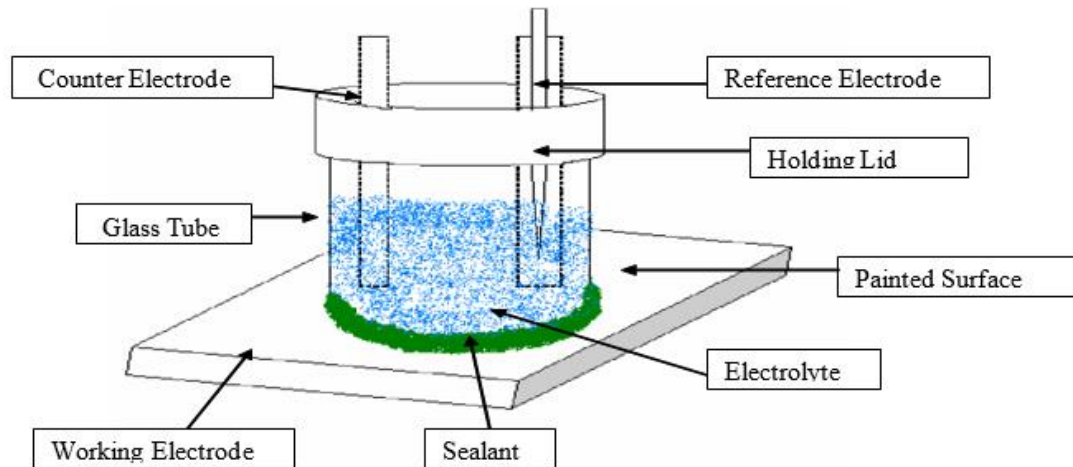


Figure 16: Cell setup for EIS[28]

Following are the basic techniques which are used in EIS:

- Potentiostatic EIS
- Galvanostatic EIS
- Hybrid EIS
- Mot-Schottky Plot

Data obtained from EIS are further analyzed using fitting models, these models are used per coating and environment type. Following information about tested material (metals, coatings) and environment can be generated[29].

- Electrolyte Resistance
- Double layer capacitance
- Polarization Resistance
- Resistance to Charge Transfer
- Coating Capacitance

Chapter 2

Literature Review

In practical world, corrosion had been most important issue. Because it keeps effecting material's life, serviceability, money and time. Since the knowing of behavior of corrosion researchers are working to understand it's chemistry, reasons of corrosion and ways to protect material from it. Therefor they were studying effect of different environments on material. Protection using electrochemistry and coatings. Some of their findings and method of investigation is summarized here.

Cheng et al. [30] In October 2016, corrosion of Q235B carbon steel was observed in sediment water of crude oil. CaCO_3 deposits were observed in greater amount over the steel surface and highly localized pitting corrosion was reported under the scale deposits. The transport of corrosion products was blocked by the scale deposits resulting in accumulation of the corrosion products. The study was conducted for 11 weeks and the corrosion rate was noted to be increased after 5 weeks of immersion.

Wang et al. [31] A research work was conducted on the corrosion of carbon steel in stagnant sea water under the influence of various deposits. Microbial and under deposit corrosion was reported. Samples were kept under deoxygenated environment with the deposits of Magnetite, calcium carbonate and sea sand for 180 days and severe corrosion was observed. Filtration and UV irradiation was used in reduction of the severity of pits while nitrate addition enhanced the corrosion very aggressively.

Y.Jafari et al. [32] In 2016, study was reported on the anticorrosion properties of polyaniline-graphene nanocomposite. Cyclic voltammetry was used to deposit the nanocomposite coating on the copper substrate. Potentiodynamic polarization and EIS was used to calculate the corrosion resistance of the coating in the aqueous solution of 5000 ppm NaCl. According to the calculations, corrosion inhibition of the coating was 98%.

Liu et al. [4] in 2010 studied stress corrosion cracking on X70 pipeline grade steel affected by strain rate in a neutral pH solution; Corrosion was analyzed by EIS and Potentiodynamic Polarization curve. On application of elastic stress and slow strain; in elastic stress, electrochemical stability didn't change but formation of small pits even in cathodic polarization was observed. This could lead to stress corrosion cracking (SCC) even in cathodically protected structure. Slow strain showed change in corrosion rate which was because of new dislocation points which were emerged and slip steps formed.

Olad et al. [33] in 2012, study was conducted on the triple hybrid system of conducting polyaniline, zinc and epoxy to evaluate their anticorrosive properties using different methodologies on metallic substrates. In the solution of 0.1M HCL, coating of nanocomposite with the thickness of 75 micro meters on iron substrate was studied. The coating was optimized for different percentages of epoxy and zinc but better results were obtained for 4 wt. % of zinc and 3-7 wt. % of epoxy. besides anti corrosive properties, epoxy and zinc also introduced mechanical strength to the nanocomposite coating. FTIR. XRD and SEM were used to characterize the coating.

Vesna [34] in 2014 coated Cu and Al with graphene and studies their electrochemical behavior. CVD was used to deposit graphene on Cu whereas on Al Coating was transferred mechanically. 0.1M NaCl solution was used as environment and EIS and Open Circuit Potential (E_{oc}) were used to check coating stability, Potentiodynamic Sweep was done to measure corrosion rate. Graphene coated Cu by CVD showed corrosion inhibiting behavior. Graphene coated Al by mechanical method showed corrosion potential as Al coated with Al oxide. Cu coated with Graphene showed better corrosion resistance than Graphene coated Al. Reason could be Al oxide instability against chloride ions when coating was ruptured.

Gomboia [3] in 2007 addressed effect of on SCC X65 steel pipeline. Pipeline sample was pressurized using water in computer control Haskel and Madan Pressurize unit. 53000 to 72% SMYS pressure cycle were applied to sample. Then sample was examined under SEM. Collinear cracks having same and different and growth angle can grow both positive and negative ways respectively. Nonlinear cracks having common growth axis can grow

and interact resulting bigger crack having new growth angle. Fatigue showed increase in SCC effect resulting failure of material.

Kumar [35] in 2008 studied corrosion behavior of Mild Steel coated with polymer and polymer-metal bilayer coating. Cyclic Voltammetry technique was used to synthesize coatings whereas EIS and Potentiodynamic corrosion testing technique were used for its study. Protection mechanism for PANI based coating was barrier but it was limited because of porous nature of PANI. In PANI-Metal bilayer coatings, metal nanoparticles filled porous sites of PANI and protection was better than PANI based, because of dual effect of barrier and sacrificial. Also, PANI-Zn based coating provided better protection than PANI-Ni.

Xu et al [36] in 2012 investigated corrosion of X100 pipeline steel under uniaxial stress conditions in NS₄ using Localized EIS. Study showed that under static load conditions corrosion potential was same as before because critical strain failure value of scale was higher than maximum strain applied on specimen. Static compressive and tensile loading didn't affect corrosion potential. Dynamic tensile loading stress would increase corrosion while compressive would inhibit. Preformed scale on steel surface, under tensile loading would create pores and increase corrosion.

Chang et al. [37] in 2012 reported on the remarkable property of PANI/Graphene composite on for the corrosion protection of steel; this composite displayed excellent barrier form the O₂ and H₂O environment in comparison with the neat Polyaniline or Polyaniline/clay composite. The composites were obtained by exfoliating and functionalizing by direct electrophilic substitution reaction in a PPA/P₂O₅ medium. After coating it on sample Tafel plots of bare steel, PANI, PANI/Graphene composite with different composition of graphene, PANI/clay composite all were tested in a 3.5 wt% NaCl electrolyte and result were compared. From Tafel plots values of E_{corr}, R_p, I_{corr}, and CR (Corrosion rate) is calculated using Stearn-Geary equation. From the test obtained it was clearly shown that how composite of PANI/Graphene shows greater corrosion resistance than any other system by proving to be effective barrier for O₂ and H₂O, Well-dispersed graphene, with a comparatively high aspect ratio compared with clay, in a polymer matrix increases the gas barrier and is accountable for the highly

wanted anticorrosion properties that make PAGCs much more efficient than PACCs.

Chang et al. [38] In 2014, studied epoxy/Graphene composite coating for corrosion resistance purpose, coated with the technique of Nano casting and data was obtained regarding corrosion prevention of this composite when it is applied on cold rolled steel. It was found that epoxy/graphene composite provide excellent corrosion resistance to 13 cold rolled steel in 3.5 wt% NaCl aqueous solution. Nano casting, which is based on the soft lithography technique, is used for the preparation of composite coating. It is a method widely used in nanofabrication by directly replicating the template to generate larger uniform patterns.

Aneja et al. [39] Study was done on the functionalized graphene coating to evaluate its barrier and protection properties when coated on mild steel. EIS was used to find out pore resistance, coating capacitance and water uptake of the coating. Experimentation was conducted at different frequencies for a certain period. Structural analysis was also studied.

Potts et al. [23] In December 2010, reported his study on graphene based polymer nanocomposite. A comprehensive study on rheological, electrical, chemical, mechanical and thermal properties was presented. Shortcomings in the processing techniques and their side effects on the properties of GO was stated. Improvement in the properties of graphene can be achieved by controlling the morphological and structural modifications. For this reason, many methods of production of Graphene are discussed here. Anticorrosion properties are substantially improved by incorporation of GO. Overall picture of properties of polymer is dependent on the intrinsic properties of GO and the way of their dispersion in the matrix. Various combination of different polymers with graphene is discussed in a comprehensive manner.

Stankovic et al. [34] In 2014 reported on graphene coatings in chloride solution and its corrosion behavior. He used chemical vapor deposition method to deposit the coating on the copper and aluminum samples. He used EIS and open circuit potential to study the electrochemical behavior of the samples. The Cu and aluminum samples were monitored in 0.1 M NaCl using different electrochemical techniques. He compared the anticorrosive

capacity of both samples. The E_{oc} value for the coated substrates of Cu was 20 mv more positive than bare samples while the current density was reduced. He observed that the coating was present even after 40 days. There was slight fluctuation in R_c value for the reason of inhomogeneous structure of graphene coating. On the other side the E_{ocp} for the coated Al sample was same as that of bare Al samples but the current density was higher. The corrosion rate was lower as compared to that of bare Al. EIS confirmed that the coating was present even after 35 days. Calculations showed that coated samples of Cu were less prone to corrosion as that of graphene coated Al samples due to mechanically transferred coating on Al samples. Higher corrosion resistance is obtained by more homogenous coating with higher purity.

Surface feature of fresh plant leaves was duplicated to develop epoxy/graphene composite corrosion inhibitors, the imprint of the leaf was transferred on the composite surface so that it shows hydrophobicity which results in corrosion protection. Electrochemical studies for corrosion, measurements were performed using Tafel plots and electrochemical impedance Spectroscopy.

Singh et al. [40] in 2012 protected Cu from corrosion in Chloride environment using graphene coating. CVD furnace was used for graphene coating. Decrease in corrosion was 1 to 2 orders of magnitude.

Singh et al. [41] in 2013 have shown in a research which involves synthesis of graphene oxide-polymer composite to test its oxidation and corrosion resistance property when coated on a copper substrate electrophoretic deposition (EPD). Electrochemical impedance spectroscopy is used for electrochemical study and to observe the corrosion protection this coating has provided to copper substrate when put in a severe chlorine ion environment. The result of the research shows that the graphene oxide – polymer composite coating has drastically reduced the corrosion rate compared to when the bare copper substrate was tested in similar environment. Polymeric isocyanate cross linked with hydroxy functional acrylic adhesive was used as polymer matrix. Hereafter polymer matrix is designated as PIHA with trade name KF-99 and Hummer's method was used for synthesis of graphene oxide.

Mondala et al. [42] in 2015 have worked on AISI 304 stainless steel, sample was used to protect it from vigorous chloride environment which can destroy the passive film of chromium oxide form on stainless steel which protect it from corrosion. In this research a nanometric composite hybrid coating is used to protect the sample, coating consisting of alternating laminate of Aluminum and titanium oxide deposited by atomic layer deposition on to a graphene layer of reduced graphene oxide. Graphene all alone was not proving sufficient to protect the passive film of SS, certain metal oxide shows more insulating property, high temperature stability and are more reactive than iron and its alloys. So, using Al_2O_3 and TiO_2 with graphene oxide have shown more corrosion resistance as compare to rGO and ceramic laminate alone. Electrochemical impedance spectroscopy (EIS) and potentiodynamic polarization technique are used for electrochemical study and to calculate the corrosion resistance.

Syed et al. [43] in year 2014 studied the corrosion protection of 316L stainless steel by using polymers multilayer coating, polyaniline-polyacrylic acid/polyethylene mine (PANI-PAA/PEI) composite coatings was prepared and coated on substrate by spin coating. The study shows in this result is that combination of coating used here provided the corrosion resistance needed when substrate was put in 3.5% NaCl environment as observed in the electrochemical measurements. The increase in corrosion resistance can be attributed to the fact that diffusion pathway of corrosion ions was increased due to multilayer structure.

Shen et al. [44] in 2005 studied corrosion protection of stainless steel sample. In this work Nano TiO_2 particles were coated on a 316L stainless steel by sol gel and dip coating method, and electrochemical test were performed to observe the corrosion resistance this coating provided to SS in chlorine environment.

Bagherzadeh et al. [45] in 2007 shows An anti-corrosive epoxy – clay nanocomposite coating was prepared and applied on metallic panels. The test was conducted in corrosive H_2O environment while salt spray and EIS method are used for corrosion test. The result shows increase in corrosion resistance when Nano clay is incorporated with epoxy coating compare with epoxy coating alone.

Shittu [46] used weight loss method to study corrosion behavior of Polystyrene coated Mild Steel. HCl and H₂SO₄ were test environments. Corrosion inhibition of Mild Steel increased at high concentration of Polystyrene but decreased with increasing time.

Raman et al. [40] in 2012 study was shown where a great amount of reduction in electrochemical degradation of copper is observed in aggressive chloride environment when copper sample were coated with graphene. Potentiodynamic Polarization and EIS test were performed for electrochemical study.

Kai QI et al.[47] In September 2015, study was conducted on the solution-process able nanocomposite of polymer grafted GO. The polymer used was polymethylmethacrylate (PMMA). This hybrid nanocomposite had the properties of permeation inhibition of GO as well as the solubility of PMMA in different solution. These qualities made it user friendly and enhanced its compatibility with various environments. Results showed the blockage of charge carriers at the metal-electrolyte transition by the coating and protected the copper metal in aggressive environment of corrosion. Atom transfer radical polymerization (ATRP) method was used in the synthesis and grafting of Nanocomposite.

Chapter 3

Experimental Work

3.1 Sample Preparation

Mild Steel of composition 0.08% C, 0.28% Mn, 0.006% Si, 0.021% P, 0.012% S, 0.021% Cr, 0.14% Cu was used for this testing. Tensile testing samples were prepared following ASTM A370 and working on lathe machine.

3.2 Tensile Test

For one sample, tensile test was performed to know about 0.5 of yield point of tensile samples. Sample dimension was such as; width 12.54mm, thickness 4.80mm, Gauge Length 50.14mm with dimension tolerance of about ± 0.2 mm. for tensile test strain rate of 2mm/minute was programmed to machine.

Surface roughness was done using 120 and 180 ambry papers followed by Phosphating for coating. Phosphating was done using Phosphoric acid (H_3PO_4) 50% by weight in distilled water. Samples were treated for 2 to 3 minutes in solution then rinsed in deionized water and dried.

3.3 PANI Synthesis

Aniline monomer from Sigma Aldrich was used for Polyaniline (PANI) synthesis.

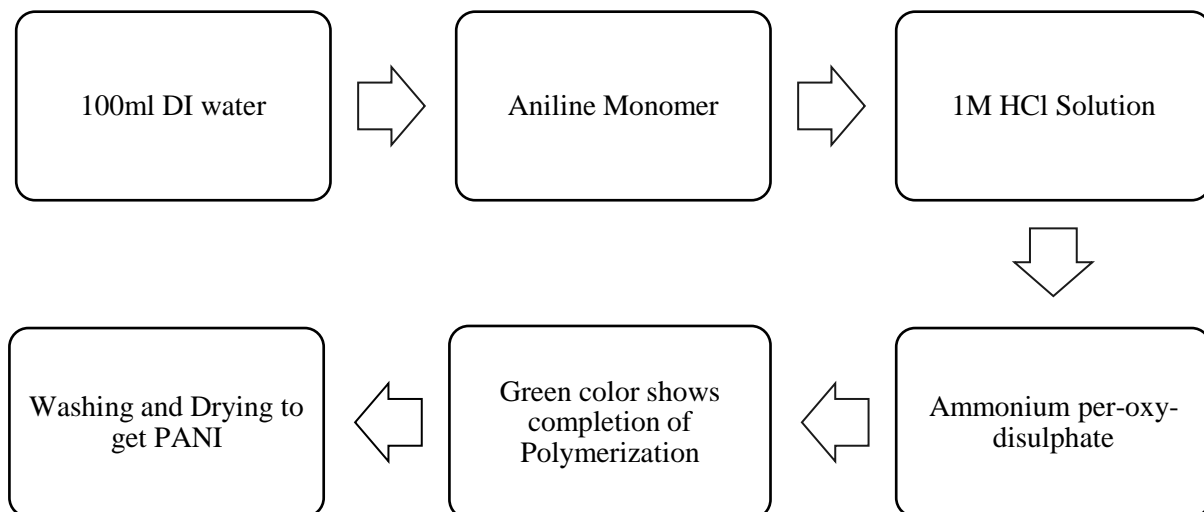


Figure 17: PANI preparation method

Chart above shows steps for PANI preparation. Aniline monomer was added to 100ml deionized (DI) water. 1mole HCl solution was slowly added and stirring is done to make aniline hydrochloride. Now in this solution Ammonium per oxy disulphate was added as initiator applied with stirring. With this addition color of solution started changing from transparent to greenish which was indication of completion of polymerization. Now solution was washed several times with DI water and then dried to get Polyaniline in powder form.

3.4 Polystyrene Coating

3g of Polystyrene (PS) was dissolved in 50ml of Toluene. Solution was put on overnight stirring on 300rpm rate. Then solution was molded into mold and metallic samples were dipped for 4 to 5 minutes each sample and air dried.

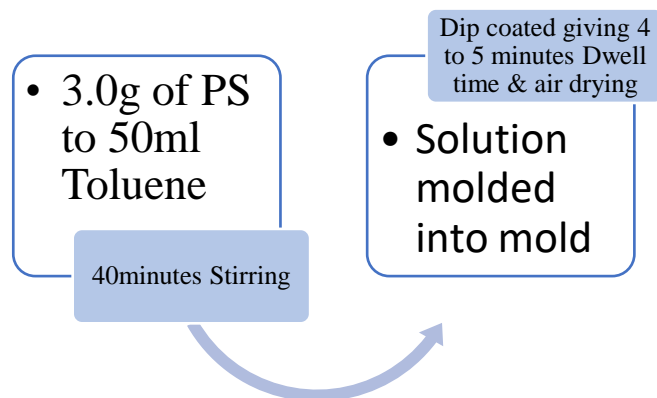


Figure 18: Polystyrene Coating Schematic Diagram

3.5 PANI-PS Polymer Blend

5% PANI-95% PS blend was prepared using Solution process method and Toluene as solvent.

To make 50ml total solution 2.85g of PS was dissolved in 25ml Toluene and was put on overnight stirring. Same method was applied on 0.15g of PANI in 25ml Toluene. After that both solutions were mixed, stirred and sonicated for two hours.

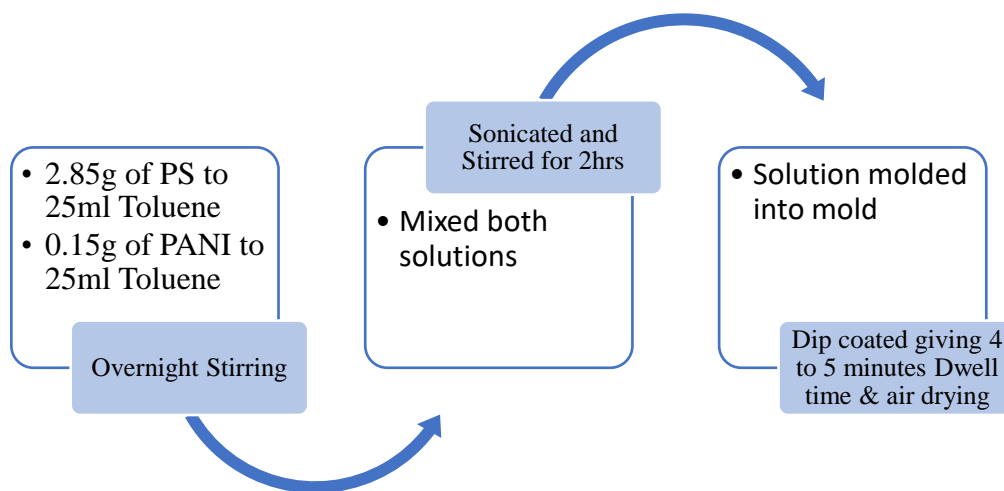


Figure 19: Polymer Blend Coating Synthesis

Then dip coating was done for 4 to 5 minutes per sample followed by air drying.

3.6 GNPs Reinforced Polymer Blend

0.015g (0.5% of 3g weight) of GNPs were added polymer blend. In this method 0.015 g GNPs were added to 10ml, 2.83g of PS to 20ml and 0.14g of PANI to 20ml Toluene. All these solutions were put on overnight stirring.

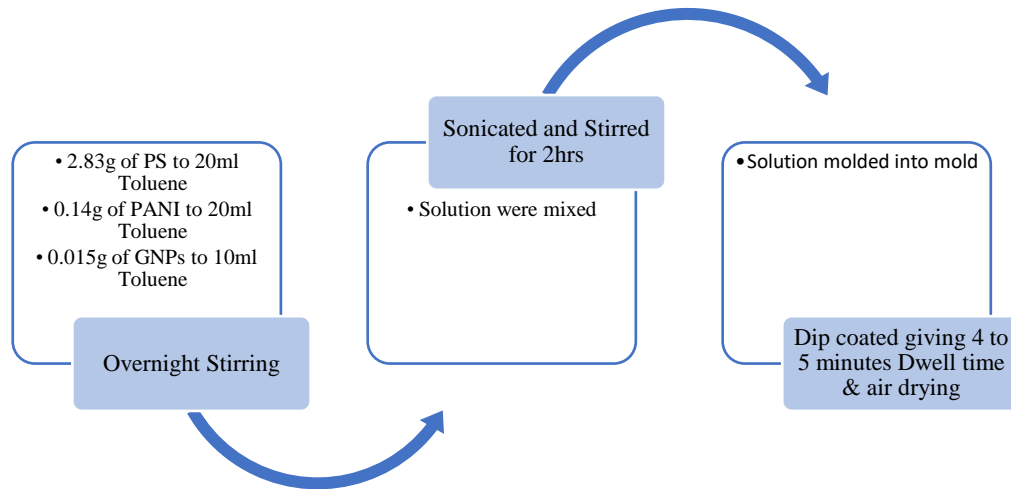


Figure 20: Nanocomposite synthesis Schematic diagram

After that all these solutions were mixed stirred and sonicated for 2 hours. After sonication solution was molded into mold and dip coating was done for 4 to 5 minutes' Dwell time for each Mild Steel sample followed by air drying.

3.7 Electrochemical Analysis of Samples

After coating MS with desired coatings two Electrochemical Analysis techniques were performed using Gamry Potentiostat manufactured by Gamry Instrument® to study corrosion behavior and to calculate corrosion related parameters.

1. Tafel Scan
2. Electrochemical Impedance Spectroscopy (EIS)

All these tests were performed in Sea water (Saline) environment, normal and uniaxial stress conditions. Shimadzu Universal testing machine was used for stress application where edges of metallic sample were insulated to avoid stray current disturbance.

3.7.1 Tafel Scan

Tafel scan is most common technique for measuring corrosion rate of metals. This technique uses DC current for corrosion measurements. Potential sweep typically ranging

-250mV to +250mV from open circuit cell potential is applied to cell in response of which cell current is measured. Data fit to result using standard Butler-Volmer Models gives estimated I_{corr} which is further used to calculate corrosion rate of metal.

3.7.2 EIS Test

EIS applies AC perturbation to test cell over applied potential and measures cell response to it. Applied potential, Frequency, Test duration and working test sample area are parameters which potentiostat requires performing this test.

Figure 17 shows data entry to perform this test.

The screenshot displays the 'Experimental Setup' tab of a software interface. The parameters are as follows:

Parameter	Value	Option
DC Voltage (V)	0.5	vs. E _{ref} (radio button), vs. E _{oc} (radio button, selected)
AC Voltage (mV rms)	10	
Test Identifier	Potentiostatic EIS	
Date	4/27/2016	
Time	12:28:36	
Initial Freq. (Hz)	100000	
Final Freq. (Hz)	0.2	
Points/decade	10	
Area (cm ²)	11.91	
Conditioning	<input type="checkbox"/> Q _{ff} 15 Time(s) 0 E(V)	
Init. Delay	<input checked="" type="checkbox"/> Q _n 10 Time(s) 0 Stab.(mV/s)	
Open Circuit (V)	-0.686014	

Figure 21: EIS Cell Setup

Three types of result graphs are generated from this test. Open Circuit Potential, Bode Plot and Nyquist Plot.

Now fitting appropriate model to these graphs gives following information about coatings.

- R_{coat} – Coating Resistance
- C_c – Coating Capacitance
- R_p – Polarization Resistance
- R_u – Uncompensated Solution Resistance
- C_{dl} – Double Layer Capacitance
- R_{pore} – Pore Resistance

3.7.3 Cell Setup

Gamry Potentiostat is based on three electrode systems;

1. Working Electrode
2. Counter Electrode
3. Reference Electrode

Figure 13 and 14 is pictorial representation of cell setup for this test.

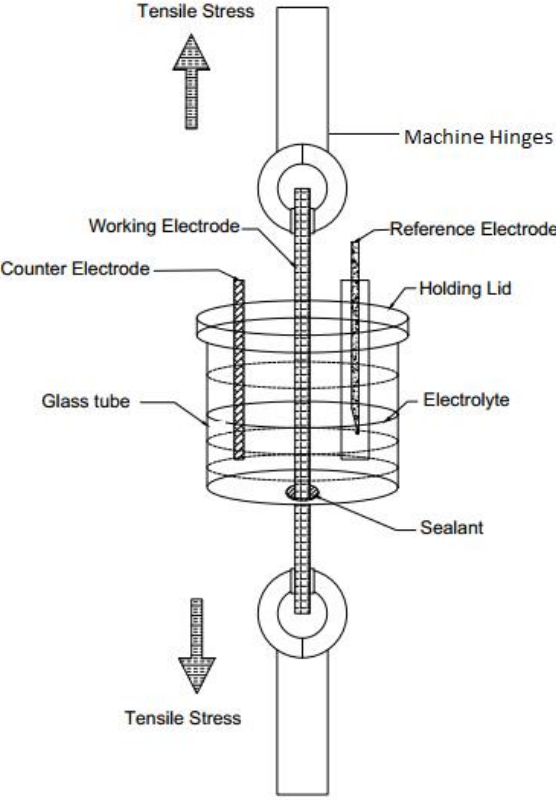


Figure 22: Test Setup Drawing



Figure 23: Cell Setup for Corrosion testing

Working Electrode (Test Sample) Among three Electrodes blue and Green wires represent Working electrode and are connected to Test Material/ Metal. Electrochemical response of this electrode is measurement of corrosion of test material.

Counter Electrode (Graphite) Counter Electrode is used to complete the circuit. Current which enters the solution through working electrode leaves the solution through counter electrode. Orange and Red wires in Gamry shows this electrode. Electrode should be inert conducting materials which in this case is Graphite.

Reference Electrode (SCE-Saturated Calomel Electrode) Potential of working electrode is measured with reference electrode which in this case is SCE. White wire in setup is connected to this electrode.

Whereas **Black Wire** in setup is ground wire.

3.8 Scanning Electron Microscopy (SEM)

SEM (JSM-6400LA) was used to characterize corroded samples. Images of both corroded and uncorroded samples at different magnifications moving from low to high were taken to investigate phenomenon of corrosion. These images also showed extent of degradation of coatings.

Chapter 4

Results and Discussion

Electrochemical test of Mild steel moving from Bare metal, Polymer (Polystyrene), Polymer blend (Polystyrene and Polyaniline) and at the end three components Nanocomposite (GNP's reinforced polymer blend) coatings was performed. Test environment for all these tests was sea water. For each type of coating another variable of stress was introduced for its effects on corrosion.

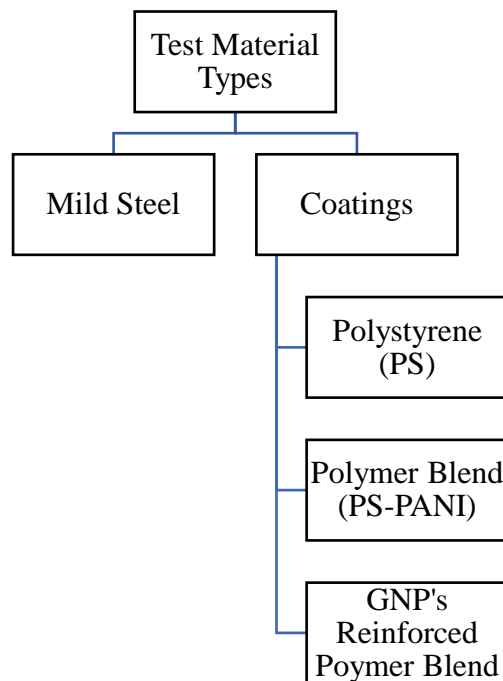


Figure 24: Material Flow Chart

4.1 Tensile Test

Following Figure 15 shows tensile test result of Mild Steel.

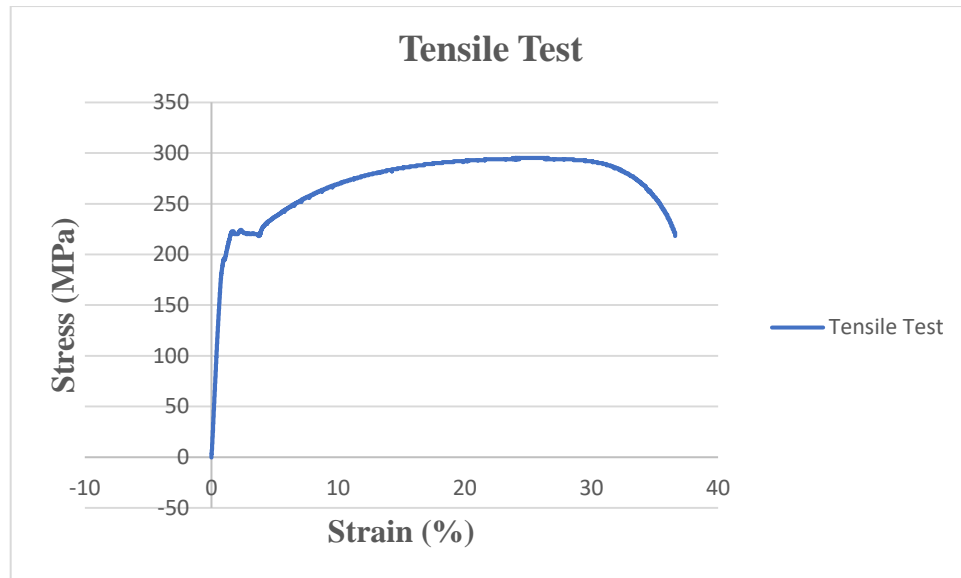


Figure 25: Stress-Strain graph of Mild Steel

From graph above value 85MPa was considered as tensile test value for Electrochemical measurements. So correspondingly value 5128N force or 85MPa stress was applied for each of coated and uncoated sample for stressed electrochemical analysis.

4.2 EIS Behavior of Capacitive Coating

To understand capacitive behavior of tested material EIS results, it would be wise to discuss pure capacitive coating behavior first. This coating has ability to store charge for a long period without degrading.

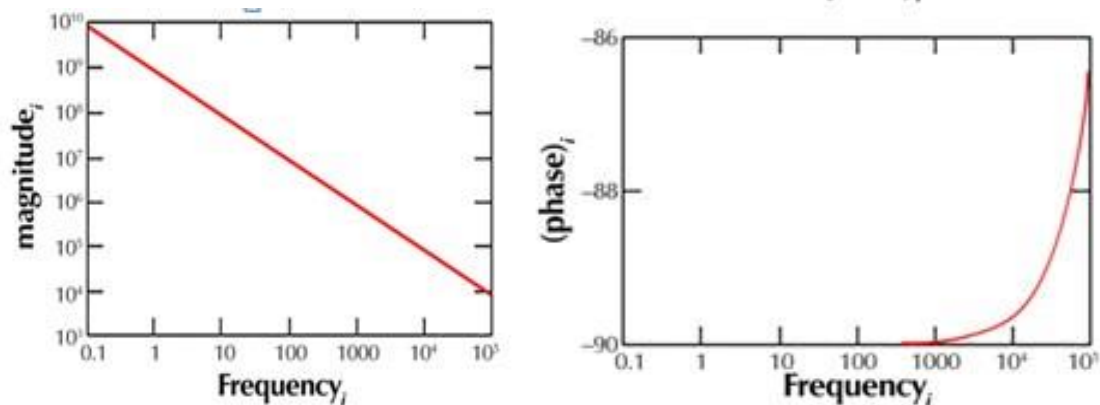


Figure 26: Bode Plot for Capacitive Coating[48]

Figure above is EIS- Bode plot showing Impedance and Phase shift response with respect to Frequency. It shows high impedance with -1 slope. Phase shift is also capacitive approaching -90° perfectly capacitive.

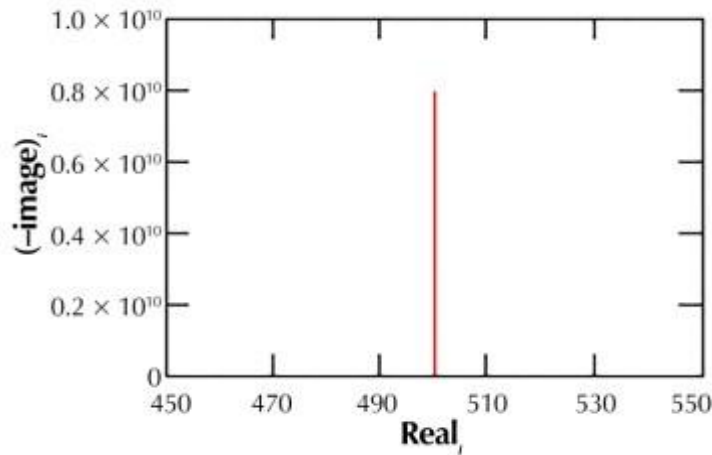


Figure 27: Nyquist Plot for Capacitive Coating[48]

EIS-Nyquist graph is between Imaginary and Real Impedance. For a coating, not perfectly capacitive shows semi-circle in this graph increasing to a maximum value and then decreasing showing coating degradation after a maximum impedance. Whereas for case above coating being perfectly capacitive it shows a straight line at 90° to Horizontal axis and showing very high Impedance to degradation.

4.3 Bare Metal

4.3.1 EIS of MS

Below is Bode presentation of EIS graph. Left vertical axis is Impedance magnitude whereas right vertical axis is phase shift. Horizontal axis show frequency. Capacitive and Impedance behavior shown here is because of Helmholtz Double Layer which is formed because of surface Metal elements and water molecules. This surface film is not protective especially in conductive electrolyte like sea water. That's why impedance of sample shown is below 10ohm. Capacitive phase shift shown in graph below goes -32° after which curve started moving upward showing that charge storage was halt at this point.

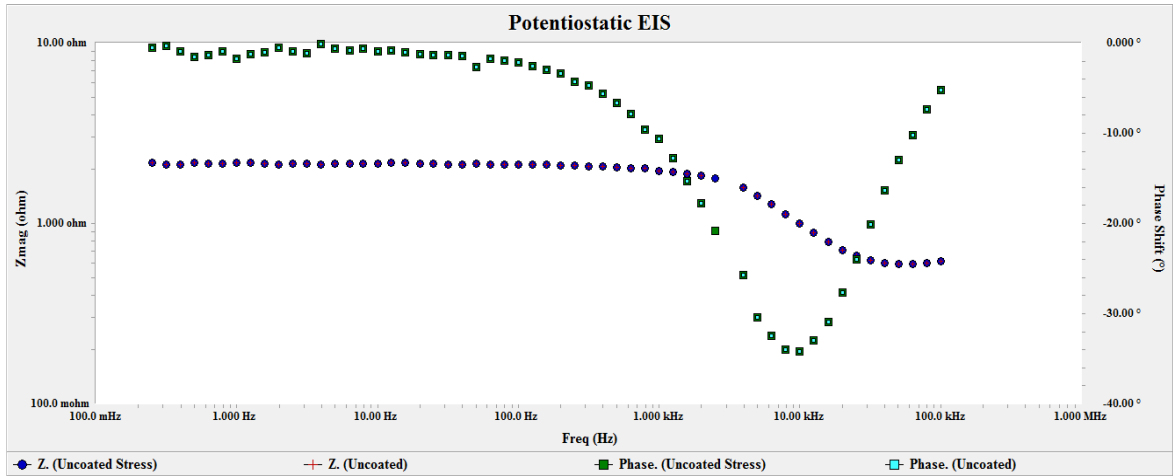


Figure 28: Bode Graph of Bare MS

Below is Nyquist presentation of EIS. Vertical axis show Imaginary Impedance and horizontal axis show Real Impedance. Result shows that impedance increased to value of 750mohm and then started descending showing charges leakage which was decrease in charge transfer resistance due to capacitive behavior of curve.

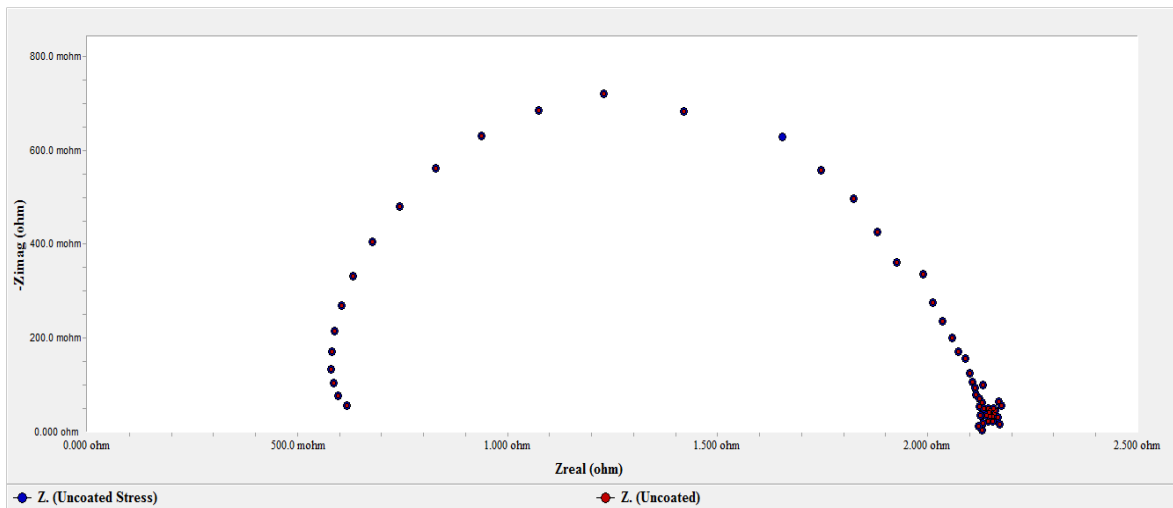


Figure 29: Nyquist Graph of Bare MS

Bode and Nyquist graphs of MS under stress are same as without stress. Which shows that for MS under this much stress level 0.5 of yield stress and sea water environment, EIS behavior is same as without stress conditions.

4.3.2 Equivalent Circuit Modelling for Bare Metal

EIS is complex mathematical phenomenon. EIS test of a bare metal or coating behaves like an electrical circuit made of resistors and capacitors. It doesn't mean that coating is made of electrical equipment's, instead metal electrodes and electrolyte behave like these electrical circuits. There are many predeveloped circuit models available in Gamry vocabulary showing corresponding coating behavior.

For a bare metal, Randles model is used which shows electrical circuit like metal behaving in electrolyte.

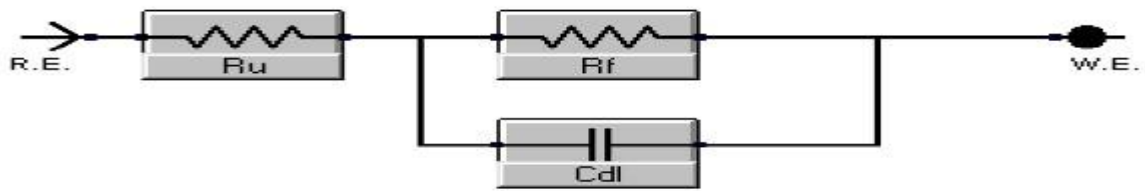


Figure 30: Circuit Model for Bare Metal[27]

This measured EIS behavior is between R.E Reference Electrode (SHE) and W.E Working Electrode (Test Metal). R_u is solution resistance acting as series resistance, C_{dl} is capacitance of double layer. This layer is because of electrolyte formed on the surface of metal. this layer has very small capacitance value. After Randel fitting following material features are observed.

Table 3:Randel Model Fitting on Bare Metal EIS Results

R_p	1.539ohm
R_u	0.577ohm
C_f	24.3 μ F

4.3.3 Tafel Scan of MS

Tafel scan is DC technique and was run after EIS. Result of Tafel Scan shows Corrosion Potential E_{corr} on Vertical axis and Log I on horizontal axis. Following figure 21 shows curve fitting of this graph and corrosion parameters.

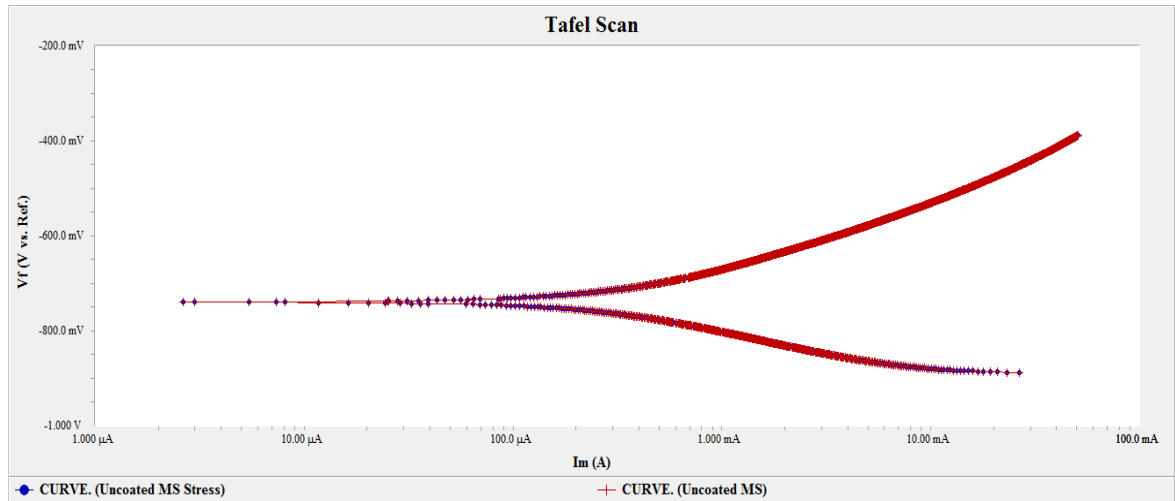


Figure 31: Tafel Scan of Bare Metal

Tafel fit of this graph showed following corrosion parameters.

Table 4: Tafel Fitting on Bare Metal Tafel Test Results

Beta A	132.9e-3 V/decade
Beta C	116.5e-3 V/decade
I_{corr}	326.0 μA
E_{corr}	-739.0 mV
Corrosion Rate	11.56 mpy

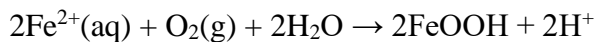
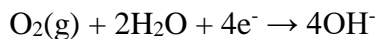
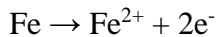
Tafel Scan for under stress showed exactly same behavior as under normal conditions. Graph fitting and corrosion parameters are just same as for case above.

Table 5: Tafel Fitting on Stresses Bare Metal Tafel Results

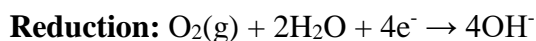
Beta A	132.9e-3 V/decade
Beta C	116.5e-3 V/decade
I _{corr}	326.0 μA
E _{corr}	-739.0 mV
Corrosion Rate	11.56mpy

4.3.4 Mechanism of Steel Corrosion

Mechanism of steel corrosion in Chloride aqueous environment has been explained in a book “Corrosion Engineering” by M. G. Fontana. There are several Oxidation and Reduction reactions involved in steel corrosion. These reactions which result rust formation are shown below[6]:



This rust doesn't have good stability on steel surface beneath it. Also, it has porosity which causes electrolyte penetration to steel. All these pores and holidays causes special type of corrosion called as Crevice corrosion. Solution remains stagnant in these sites. In Sea water (Chloride environment) general dissolution of metal and reduction of oxygen occurs as shown below for metal as M.



Initially dissolution is same on surface and crevices but after certain time there is depletion of Oxygen in crevices. With passage of time this effect gets severe by increasing Metal

positive ions in crevices and to neutralize this effect Chloride ions from solution migrate into crevices. This effect even increases corrosion rate inside the crevices[6].

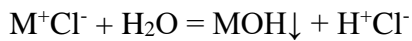


Figure 25 is pictorial representation of this reaction.

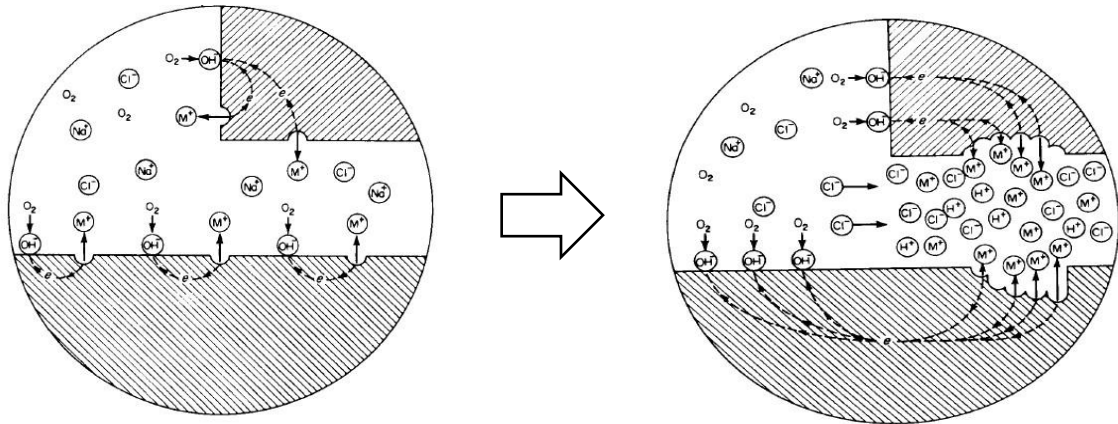


Figure 32: Pictorial Presentation of Crevice Corrosion[6]

4.4 Polystyrene (PS)

4.4.1 EIS of PS Coated MS

EIS behavior of PS coated Mild steel is shown in figure below:

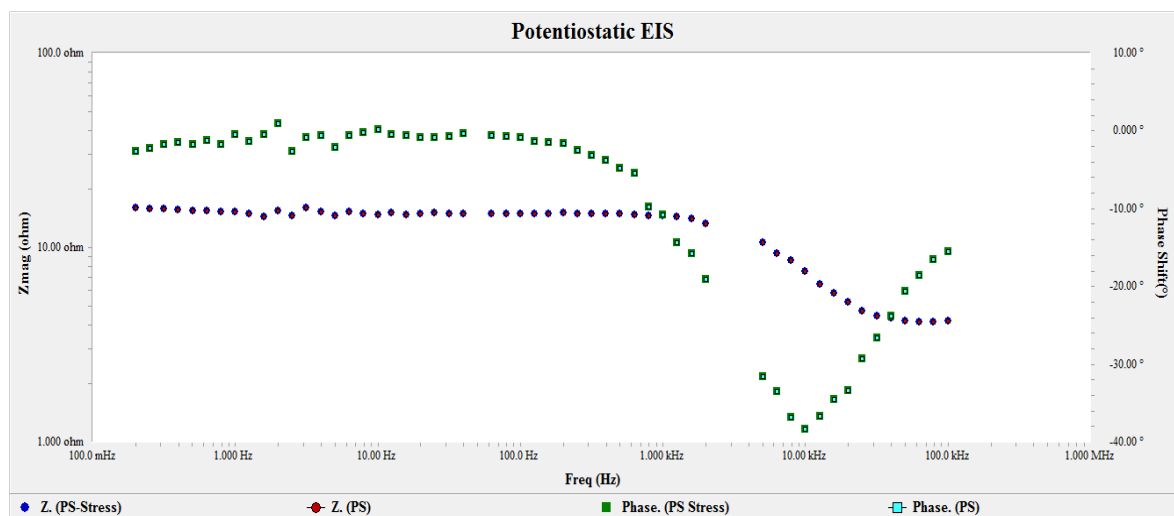


Figure 33: Bode Plot Showing EIS of PS coated MS

Graph shows capacitive behavior of coating between 1KHz and 10KHz frequencies. Whereas impedance for this coated sample is slightly higher than bare mild steel sample. Increase in impedance will also be evident from Nyquist plot shown below. From this result phase shift is at about -38° . After which curve again started going up showing charges leakage at this point.

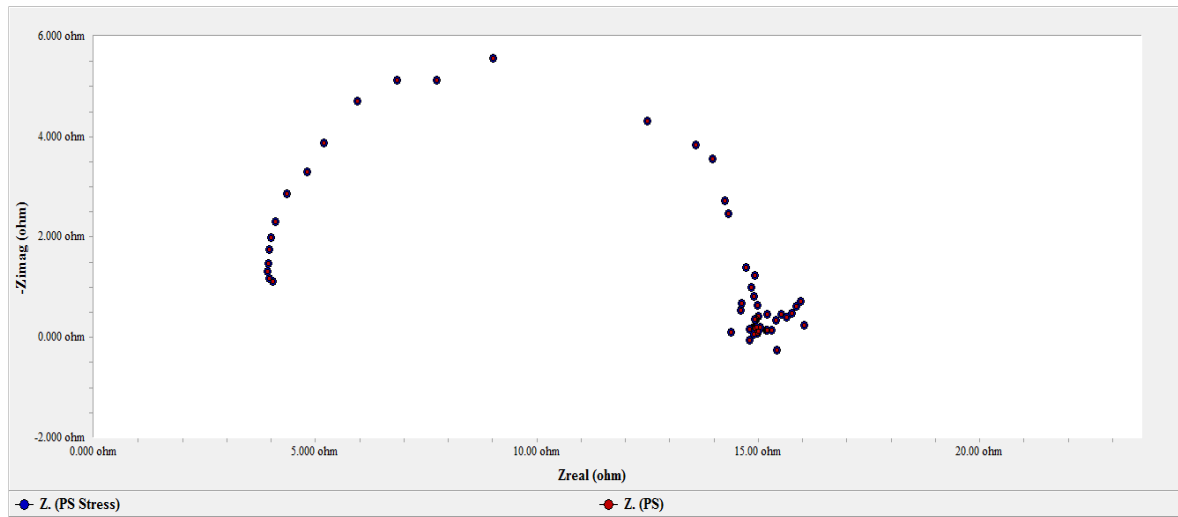


Figure 34: Nyquist Plot showing PS coated MS

Plot above shows that coating protected to a value of 6ohm Impedance and then started degradation. This result shows that this coating provided better impedance and charge storage than Bare Steel.

Bode and Nyquist graphs of PS coated under uniaxial stress were just same as without stress case. This result showed that at this much stress on bare metal PS is not getting damaged and showing same behavior.

4.4.2 Equivalent Circuit Modeling for Coated MS

As discussed earlier an electrical circuit can represent EIS behavior of a metal. Randel model showed this behavior of Bare metal but for a coating it won't be that simple. Following circuit diagram shows and Electric circuit responding like a coating.

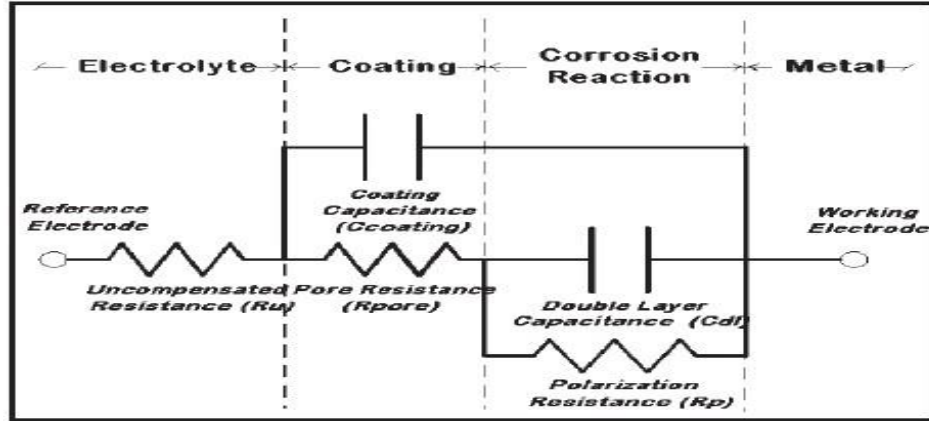


Figure 35: Circuit Model Representing Coating[48]

Figure above is clearly labelled about each resistor and capacitor representing which part of coating. Now to obtain coating parameters these models are applied on results. Model giving best curve fitting depicts best coating behavior. There are many circuits models already present in Gamry and even circuit of one's own choice can be made in it. For this coating REAP2CPE model was applied. In response to which it showed following results.

Table 6: Reap2CPE Model Fitting on PS Coated MS EIS Results

R_{soln}	228.8e-9ohm
R_{corr}	11.50ohm
R_{po}	3.641ohm
C_{cor}	4.682e-6F
C_c	4.721e-9F

From here R_{po} is Pores Resistance whereas C_c is Coating Capacitance. Both are very important features in terms of coating protection. To understand their effect to coating stability and metal protection, R_{po} directly gives information about coating stability. Higher R_{po} refers to higher strength and stability of coating. Whereas Coating capacitance (C_c) has inverse relation with total Impedance of coating. Such as shown here in a relation:

$$Z = 1/2\pi fC \text{ [27]}$$

Where Z is Impedance, f is Frequency C is capacitance of coating.

4.4.3 Tafel Scan of PS Coated MS

Following graph shows Tafel results for Polystyrene Coated Mild steel under normal conditions.

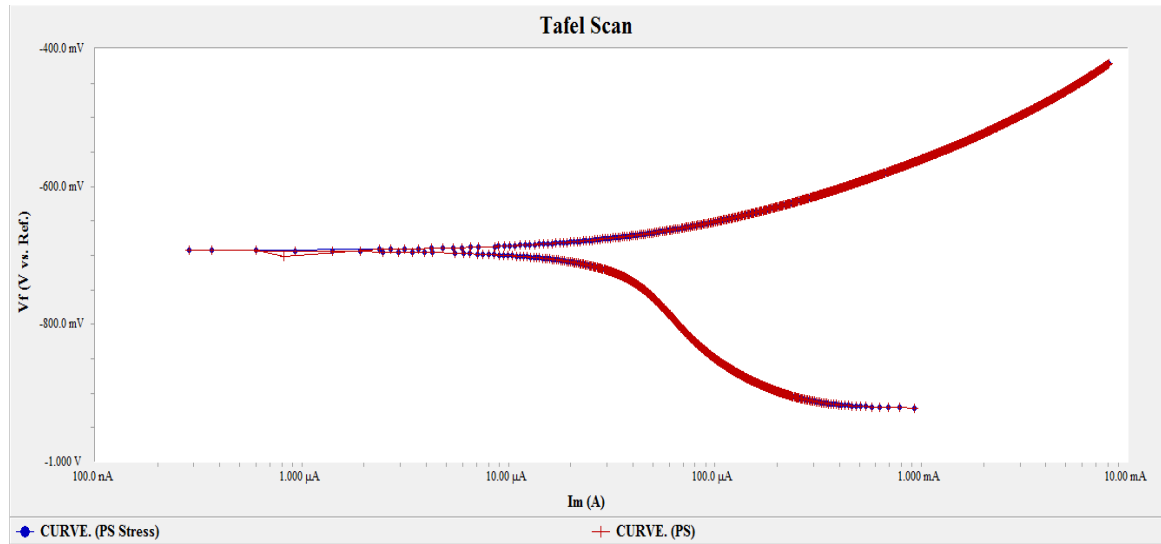


Figure 36: Tafel Scan of PS coated MS

Table 7: Tafel Fitting on PS Coated MS Tafel Scan Result

Beta A	106.4e-3 V/decade
Beta C	1.000e15 V/decade
I_{corr}	68.00 μ A
E_{corr}	-693.0 mV
Corrosion Rate	2.567mpy

Tafel scan of PS coated MS under Stress showed Tafel Scan results just as without stress case. This shows that stress applied on base metal didn't rupture coating and coating was protecting metal as case without stress.

Table 8: Tafel Fitting on PS Coated MS Stresses Tafel Scan Result

Beta A	106.4e-3 V/decade
Beta C	1.000e15 V/decade
I_{corr}	68.00 μ A
E_{corr}	-693.0 mV
Corrosion Rate	2.567mpy

4.4.4 SEM of PS Coated Steel

SEM images of PS coated steel before and after corrosion are shown below:

Before Corrosion

After Corrosion

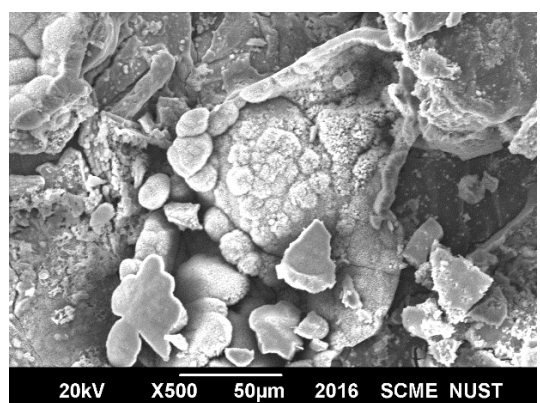
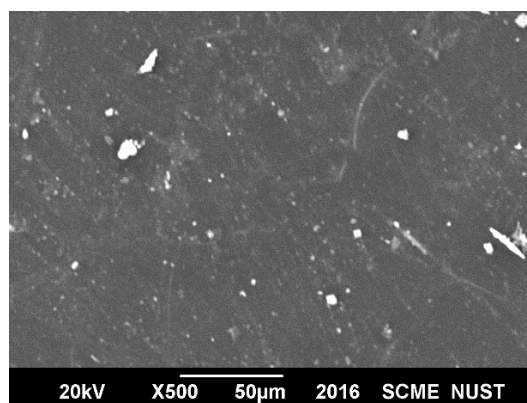
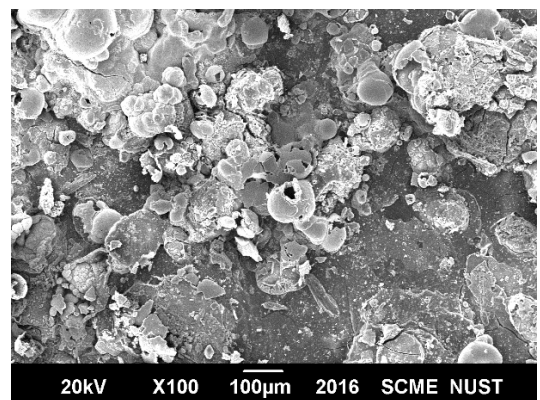
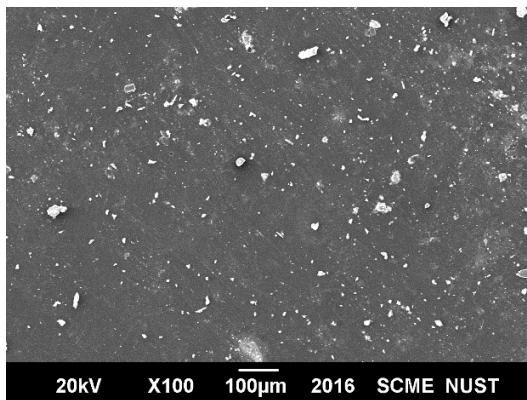


Figure 27: SEM Images of PS Coated Steel

Images above show clear difference in surface deformation because of corrosion. Gradual increase in magnification does shown change in surface appearance. After corrosion micrographs show corrosion products formed after interaction of coating with electrolyte. However, it does not show any coating damage if occurred because of corrosion. But it does show formation of corrosion products during electrochemical analysis.

4.5 PANI-PS Polymer Blend Coating

4.5.1 EIS of Polymer Blend Coated MS

EIS behavior of Polymer blend coated MS is shown below.

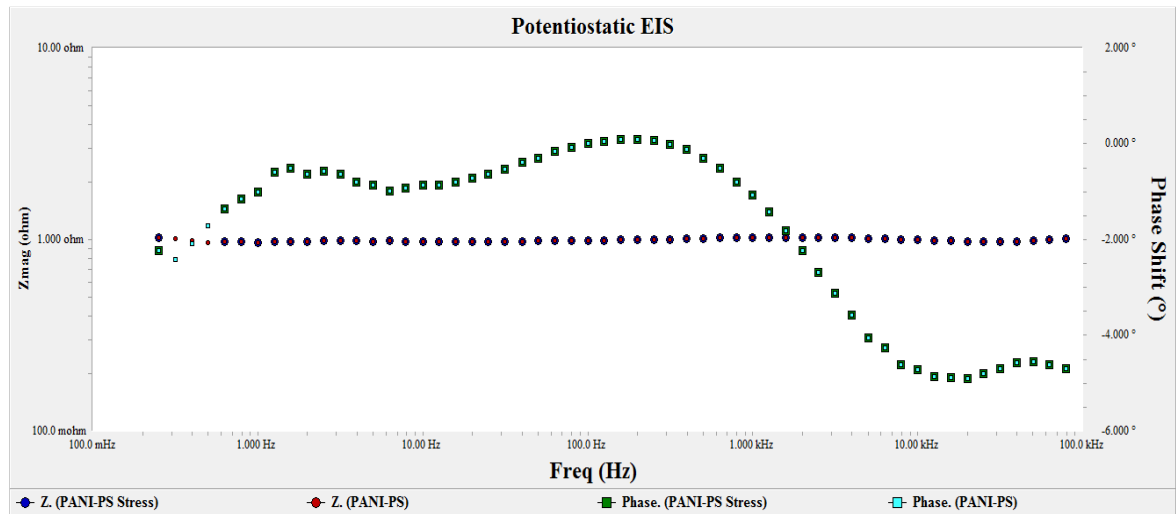


Figure 37: Bode Plot Showing PANI-PS Polymer Blend Coated MS

Result shows that over the change of frequency there was no appreciable change in Impedance. This shows that coating was showing more resistive behavior in this environment than capacitive behavior. Phase shift of -5° only was observed from results.

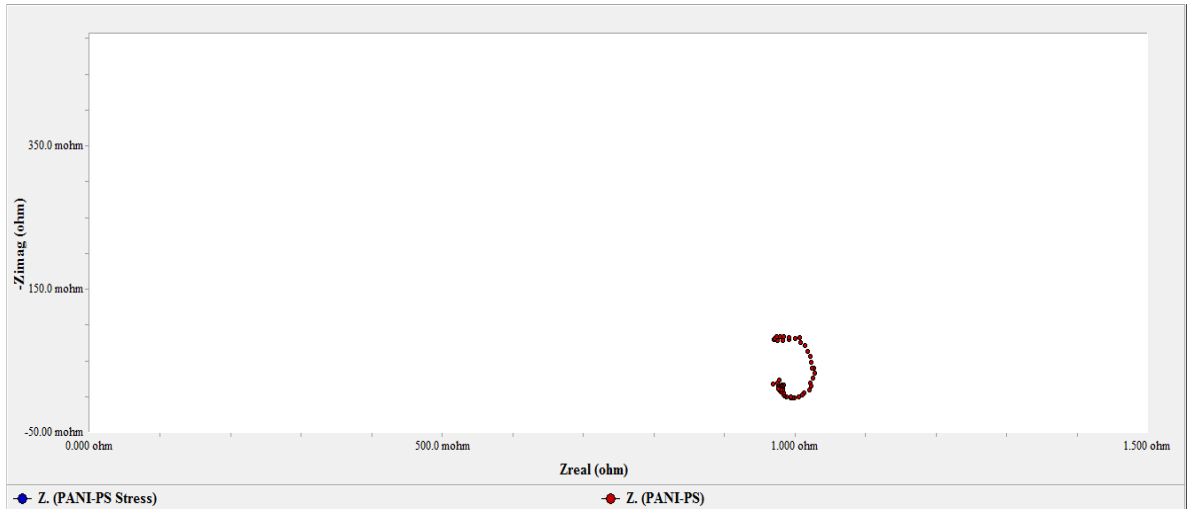


Figure 38: Nyquist Plot Showing PANI-PS Polymer Blend Coated MS

Nyquist further showed this resistive behavior. Coating showed impedance of only 125mohm. This shows that charge storing capability in this coating was smaller than PS coating. This curve behavior is also unstable one in terms of EIS study. EIS pattern of this coating for both stress and normal conditions was just same.

4.5.2 Mechanism of EIS and Circuit Modelling

By applying REAP2CPE model following EIS parameters were calculated.

Table 9: Reap2CPE Model Fitting on PANI- PS Blend Coated MS EIS Results

R_{soln}	72.60e-6ohm
R_{corr}	732.5e-3ohm
R_{po}	265.2e-3ohm
C_{corr}	22.61e-6F
C_c	145.4e-9F

4.5.3 Tafel Scan of PANI-PS Polymer Blend Coated MS

Tafel Scan of Polymer blend are shown below:

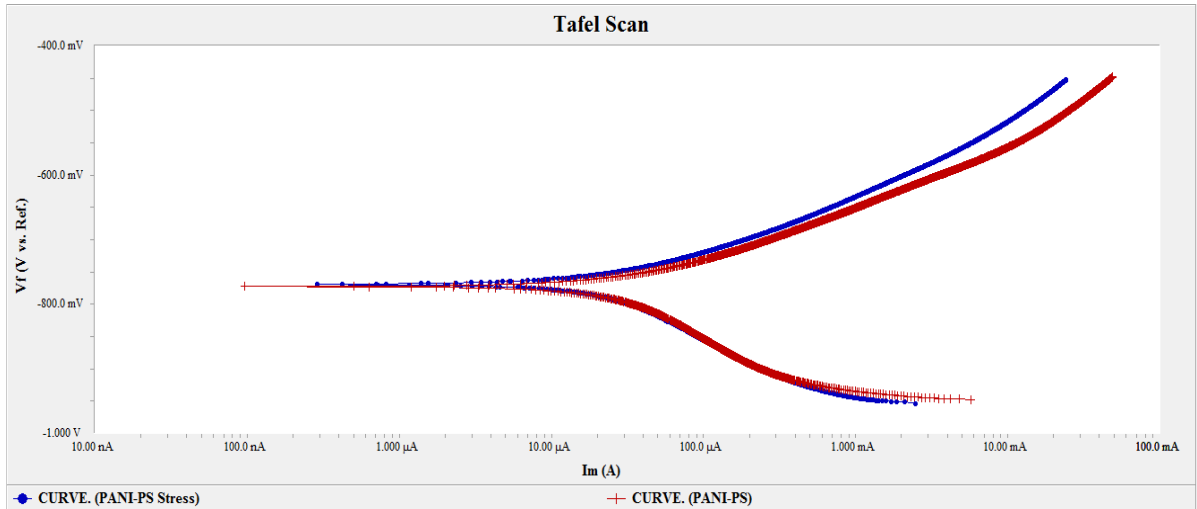


Figure 39: Tafel Scan PANI-PS Polymer Blend Coated MS

Table 10: Tafel Fitting on PANI- PS Coated MS Tafel Scan Result

Beta A	85.70e-3 V/decade
Beta C	175.0e-3 V/decade
I _{corr}	30.30 μ A
E _{corr}	-769.0 mV
Corrosion Rate	1.065 mpy

Same as for previous cases this coating didn't rupture under applied stress and showed same corrosion behavior as without stress cases. So, same result and result parameters shown by material are shown here.

Table 11: Tafel Fitting on PANI-PS Coated MS Stresses Tafel Scan Result

Beta A	89.80e-3 V/decade
Beta C	324.9e-3 V/decade
I _{corr}	46.40 μ A

E_{corr}	-772.0 mV
Corrosion Rate	1.627Mpy

4.5.4 SEM of PANI- PS Polymer Blend Coated MS

SEM images below show PANI-PS polymer blend coated steel before and after Corrosion.

Before Corrosion

After Corrosion

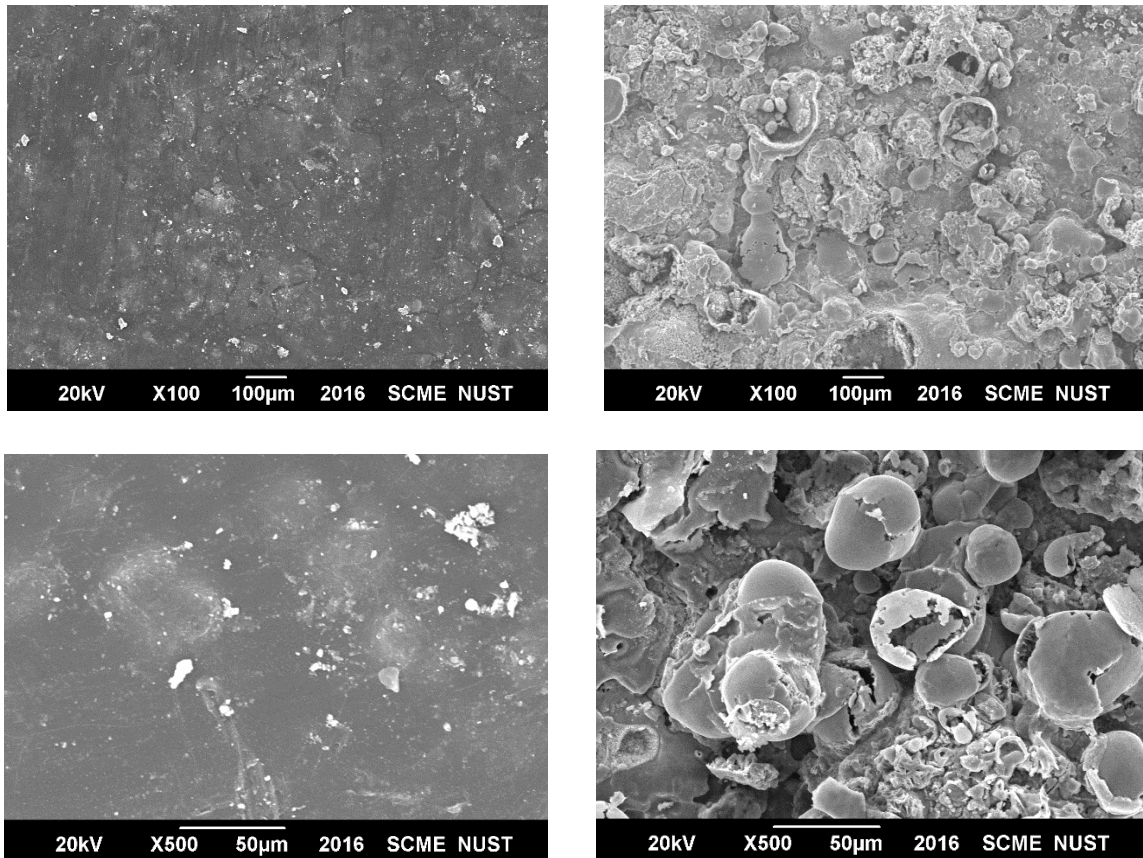


Figure 30: SEM Images of PANI-PS Coated Steel

Above SEM images show that corrosion reaction caused blisters in coating. These bubbles/blisters are result of water penetration into polymeric coating. Also, it shows reaction between ions present in sea water and polymeric material. This reaction has caused corrosion products which are showing featured texture in after corrosion SEM micrographs.

4.6 GNP's Reinforced Polymer Blend (Tri-component) Coated MS

4.6.1 EIS of GNP's Reinforced Polymer Blend Coated MS

Following Figure shows EIS results from experiment.

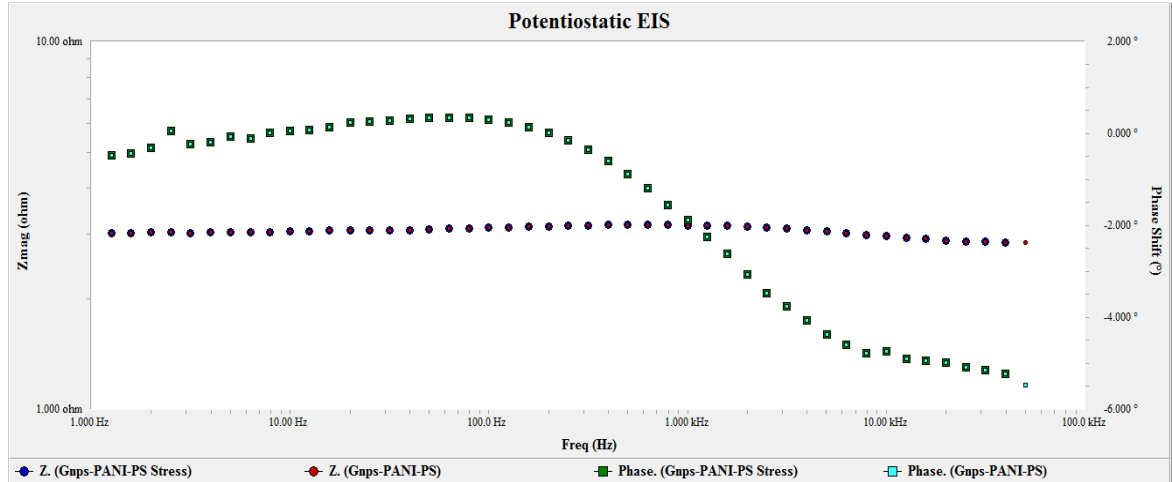


Figure 40: Bode Result of GNP's Based Polymer Blend

EIS result of this coating shows that in sea environment it acted like a resistor. Upon frequency sweep, material didn't show change in resistance which is the property of resistor. Just like in case of PANI -PS polymer blend here GNP's and PANI behaved as charge transfer source. This easiness in charge transfer caused decrease in capacitance of material.

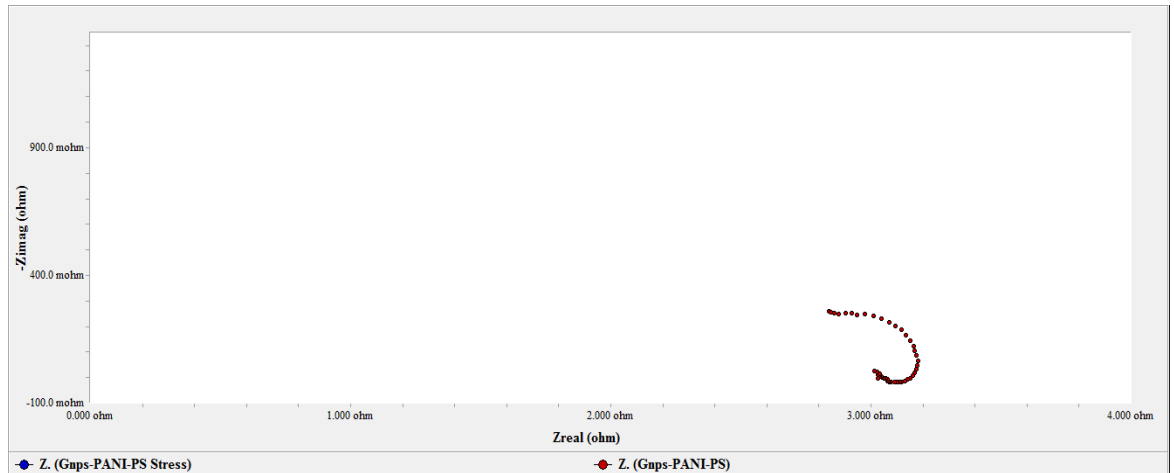


Figure 41: Nyquist Plot for GNP's Reinforced Polymer Blend Coated Under Stress

Above result shows that under stress EIS pattern of material was just same. This shows stability of coating under stress. This continuity in coating behavior is important for application where stress is applied on base material. Because it will be able to protect material even in that case.

4.6.2 Mechanism of EIS and Circuit Modelling

For this again REAP2CPE model was applied as for coatings before. Following are results shown from those this model fitting which give further information about coatings.

Table 12: Reap2CPE Model Fitting on GNP's- PANI- PS Coated MS EIS Results

R_{soln}	2.240e-6ohm
R_{corr}	3.035ohm
R_{po}	33.46e-3ohm
C_{corr}	20.00e-6F
C_c	163.5e-9F

From these values coating showing good capacitive properties have important features of R_{po} and C_c . whereas here this case is different.

4.6.3 Tafel Scan of GNP's Reinforced Polymer Blend Coated MS

Below Tafel Scan results of GNPS's Reinforced Polymer Blend coated MS are shown.

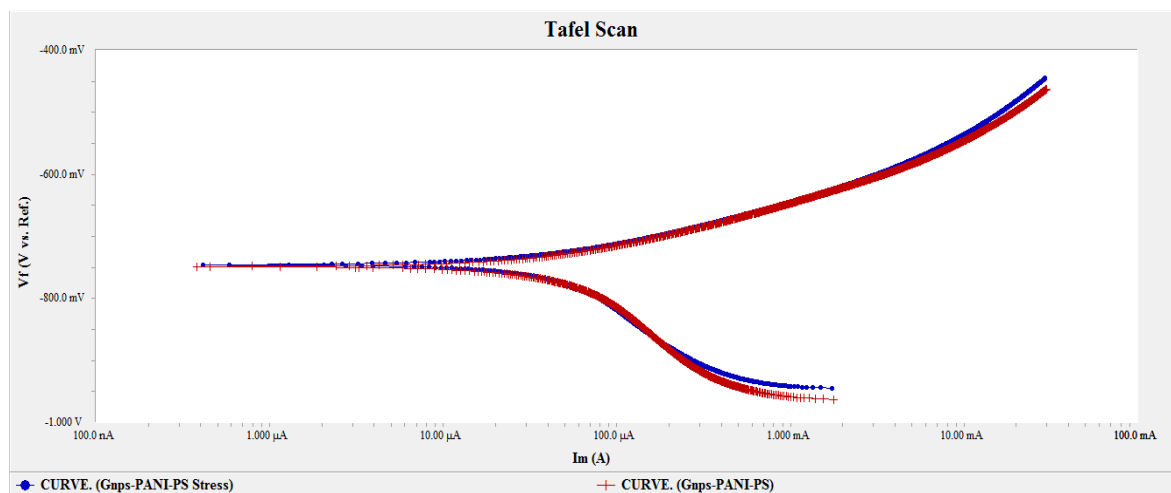


Figure 42: Tafel Scan of GNP's Reinforced Polymer Blend Coated MS

Table 13: Tafel Fitting on GNP's-PANI- PS Coated MS Tafel Scan Result

Beta A	71.10e-3 V/decade
Beta C	124.3e-3 V/decade
I _{corr}	40.70 μA
E _{corr}	-749.0 mV
Corrosion Rate	1.563 mpy

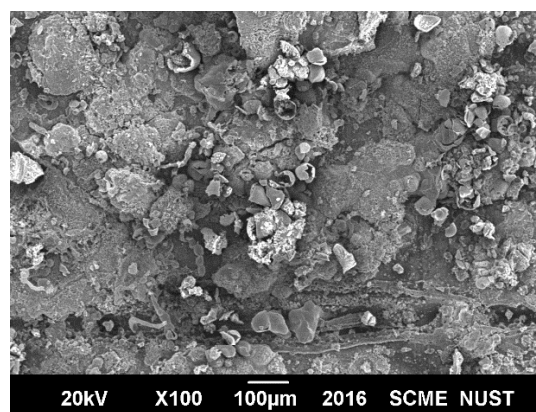
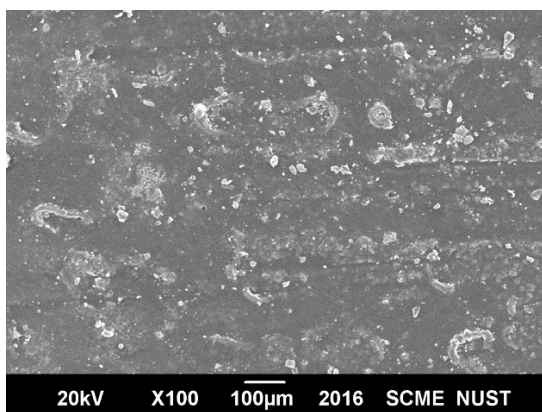
Table 14: Tafel Fitting on GNP's-PANI- PS Coated MS Stressed Tafel Scan Result

Beta A	71.40e-3 V/decade
Beta C	147.0e-3 V/decade
I _{corr}	41.40 μA
E _{corr}	-746.0 mV
Corrosion Rate	1.558Mpy

4.6.4 SEM of GNPS's Reinforced Polymer Blend Coated MS

Before Corrosion

After Corrosion



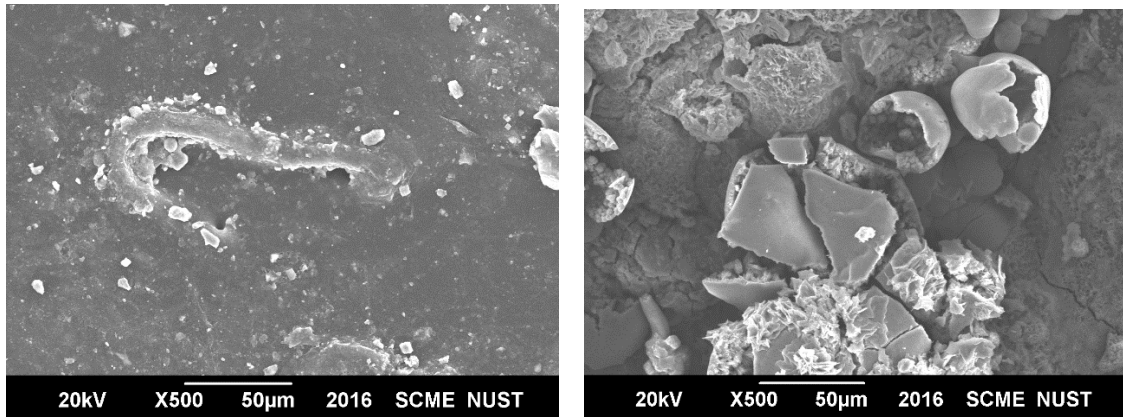


Figure 33: SEM Images of GNP's Reinforced Polymer blend Coated MS

Images above in figure 33 are clear illustration of corrosion effects. at even low magnification X100 many corrosion products can be seen which are result of corrosion reaction of very active ions present in electrolyte. As sea water, which carry vigorous reactive ions was testing medium. These ions reacted with exposed coating to environment and resulted these products.

All after corrosion SEM micrographs above show corrosion products which are reason of water and water dissolved ions interaction with base polymer which is PS. PANI and GNP's do not show any distinct feature appearance in SEM micrographs.

4.7 Comparative Result of EIS

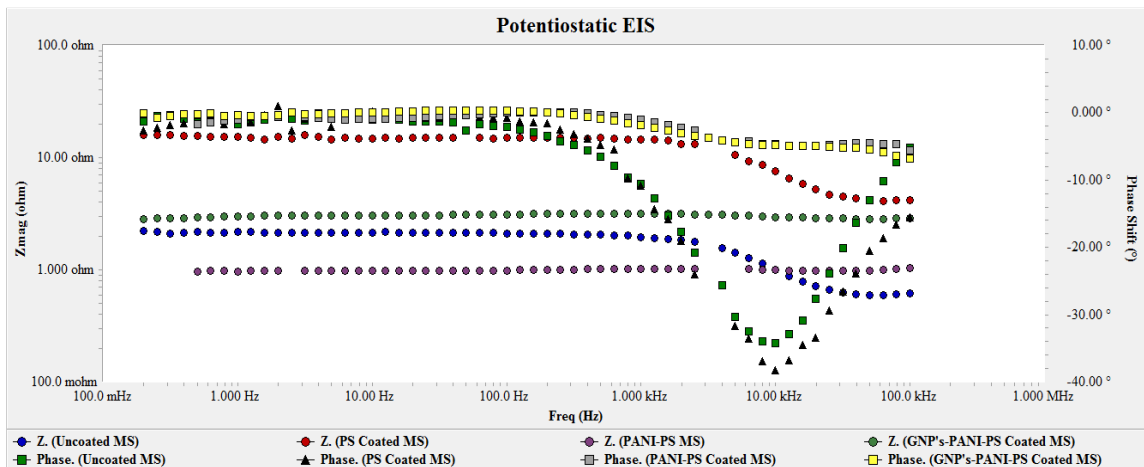


Figure 43: Comparative Result of EIS

Comparative results in figure 33 illustrate that with the addition of PANI AC impedance of coating is decreased. Because PANI acted as conductive source and charge carrier in this case. Addition of GNP's to polymer blend cancelled the impedance effect of PANI and increased impedance to higher side but it was still lower than the case of PS coating. Whereas changing in coating behavior from capacitive to resistive because of PANI was same in in polymer blend and nanocomposite.

4.8 Comparative Result of Tafel Scan

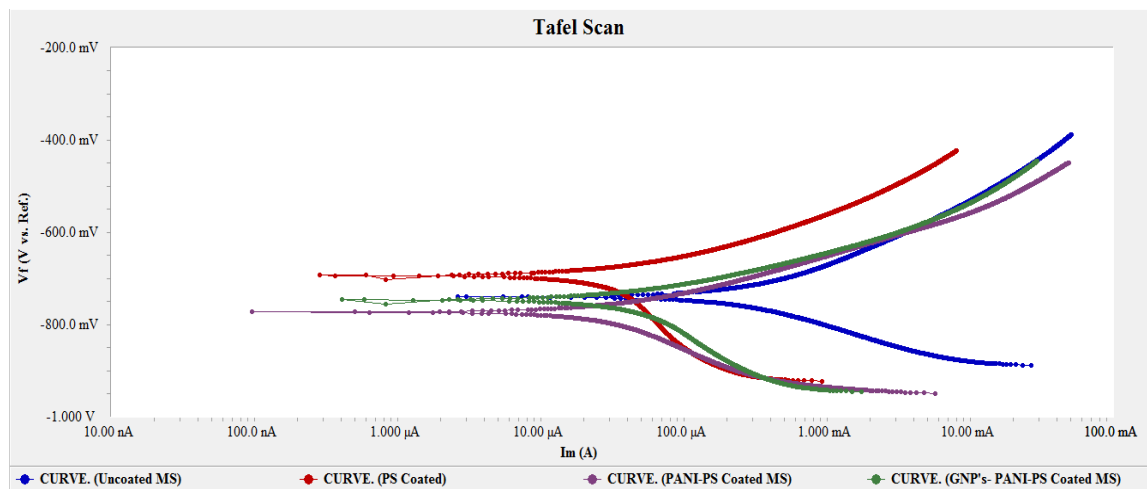


Figure 44: Comparative Result of Tafel Scan

In Tafel comparison figure 34, result showed that PS has higher corrosion potential that PANI added polymer blend and nanocomposite. Decrease in potential in polymer blend nanocomposite was because of conductive effect of PANI. Whereas at the same time PANI addition further showed decrease in current density and corrosion rate.

Polystyrene acts as barrier between metal substrate and corrosive medium. This is the main reason of corrosion protection[46]. Yu et al [49] addressed that in saline solution polystyrene as coating shifts corrosion potential of mild steel to anodic direction with decrease in current density and corrosion rate. Same has happened in this case. Bode result showed high pore resistance. Change in impedance over change in frequency depicting polarization and charge storage (capacitive) behavior of polystyrene. Higher phase shift in PS also attributes this fact [50][51].

PANI provides passive layer corrosion protection. Its porous nature can lead to a decrease in corrosion potential with small exposure time[35][52]. But still shows very low corrosion rate same has happened in this case in PANI Tafel Scan results. With addition of PANI to PS, porosity in PANI leads to a decrease in corrosion potential at the same time also decrease in corrosion rate. In saline environment, galvanic coupling of PANI with mild steel leads to compounds blocking pinholes and further corrosion reaction[53]. Mostafaei [52] explained this by PANI intercepting electrons transfer between metal and environment. Corrosion protection is because of reduction of PANI-emeraldine salt to PANI-Leucosalt with release of sulphonic ions. Iron ions react with sulphonic ions to make passive layer, whereas PANI-leucosalt oxidizes back to PANI-emeraldine by reacting with oxygen present in the environment. This is kind of self-healing phenomenon. With addition of PANI to PS AC conductivity of PS is increased as shown in bode result figure 6[54]. This increase in conductivity decreases the chances of charges to store and leads to stability in impedance over change in frequency[50][51].

Graphene coatings being hydrophobic and having high oxidation potential can protect metal substrates from corrosion[55]. In polymer based coatings it shifts corrosion potential to noble direction and decrease corrosion density. In this case addition of GNP's to PANI-PS has relatively shifted the corrosion potential to positive direction catering the effect of decrease in potential because of PANI porosity. At the same time showing less current density and corrosion rate. In bode results it shows slight increase in impedance to AC charge transfer. Stability in impedance remained so because of PANI also very low phase angle showed conductivity of coating. Overall low impedance and pore resistance values in all three coating depict non-homogeneous coatings thickness but results show the behavior of coatings[52][56]. For all coatings at 85MPa applied stress EIS and Tafel scan showed same behavior which shows that at applied stress generated strain was not enough to break coatings mechanically[3][36].

Conclusions

1. Electrochemical Impedance Spectroscopy (EIS) of bare steel showed very low impedance to charge transfer 750mohm and Phase shift of -32° . Whereas PS coating showed better impedance as 6ohm and higher Phase shift of -40° . With the addition of PANI and GNP's charge transfer resistance was decreased and coating acted as a resistor which is not being affected by change in frequency.
2. Corrosion rate addressed by Tafel Scan showed relatively high corrosion rate for bare steel as 11.56mpy. PS coated MS showed 78% decrease in corrosion rate. PANI-PS polymer blend coated MS further reduced corrosion rate to 86% and GNP's reinforced PANI-PS polymer blend coated MS decreased corrosion rate as 87%.
3. In stressed and unstressed conditions for all above coated and bare steel samples EIS and Tafel Scan showed same results. This shows that for stressed bare MS surface was behaving same as unstressed case. For coated sample, strain at applied stress was not enough to break coatings at any point and coatings were providing corrosion protection at that stress level.
4. SEM as qualitative analysis showed corrosion products in polymer which were same in all three coatings. This showed that because of environment same kind of electrochemical reaction occurred. PANI and GNP's did not show any distinct feature in after corrosion samples results.

References

- [1] W. D. Callister and D. G. Rethwisch, *Fundamentals of Materials Science and Engineering: An Integrated Approach*. John Wiley & Sons, 2012.
- [2] F. Atmani, D. Lahem, M. Poelman, C. Buess-Herman, and M.-G. Olivier, "Mild steel corrosion in chloride environment: effect of surface preparation and influence of inorganic inhibitors," *Corros. Eng. Sci. Technol.*, vol. 48, no. 1, pp. 9–18, Feb. 2013.
- [3] E. Gamboa, V. Linton, and M. Law, "Fatigue of stress corrosion cracks in X65 pipeline steels," *Int. J. Fatigue*, vol. 30, no. 5, pp. 850–860, May 2008.
- [4] Z. Y. Liu, X. G. Li, and Y. F. Cheng, "Effect of Strain Rate on Cathodic Reaction During Stress Corrosion Cracking of X70 Pipeline Steel in a Near-Neutral pH Solution," *J. Mater. Eng. Perform.*, vol. 20, no. 7, pp. 1242–1246, Oct. 2010.
- [5] "Types of Corrosion." [Online]. Available: http://corrosion-protect.com/library_types_of_corrosion.php. [Accessed: 04-Jan-2017].
- [6] M. G. Fontana, *Corrosion Engineering*. Tata McGraw-Hill Education, 2005.
- [7] S.-W. Kuo and F.-C. Chang, "POSS related polymer nanocomposites," *Prog. Polym. Sci.*, vol. 36, no. 12, pp. 1649–1696, Dec. 2011.
- [8] I. Zaman, B. Manshoor, A. Khalid, and S. Araby, "From clay to graphene for polymer nanocomposites—a survey," *J. Polym. Res.*, vol. 21, no. 5, p. 429, May 2014.
- [9] V. Thirtha, R. Lehman, and T. Nosker, "Morphological effects on glass transition behavior in selected immiscible blends of amorphous and semicrystalline polymers," *Polymer*, vol. 47, no. 15, pp. 5392–5401, Jul. 2006.
- [10] A. Franck, "Mixing Rules for Complex Polymer Systems," *tainstruments*, 05-Jan-2017..
- [11] V. Thirtha and R. Lehman, "Glass transition effects in immiscible polymer blends (PDF Download Available)," *ResearchGate*. [Online]. Available: https://www.researchgate.net/publication/265489521_Glass_transition_effects_in_immiscible_polymer_blends. [Accessed: 13-Apr-2017].
- [12] W. J. Bae, W. H. Jo, and Y. H. Park, "Preparation of polystyrene/polyaniline blends by in situ polymerization technique and their morphology and electrical property," *Synth. Met.*, vol. 132, no. 3, pp. 239–244, Jan. 2003.
- [13] T.-Y. Chu et al., "Bulk Heterojunction Solar Cells Using Thieno[3,4-c] pyrrole-4,6-dione and Dithieno[3,2-b:2',3'-d]silole Copolymer with a Power Conversion Efficiency of 7.3%," *J. Am. Chem. Soc.*, vol. 133, no. 12, pp. 4250–4253, Mar. 2011.
- [14] "Polystyrene," *Wikipedia*. 13-Dec-2016.
- [15] J. Maul, B. G. Frushour, J. R. Kontoff, H. Eichenauer, K.-H. Ott, and C. Schade, "Polystyrene and Styrene Copolymers," in *Ullmann's Encyclopedia of Industrial Chemistry*, Wiley-VCH Verlag GmbH & Co. KGaA, 2000.
- [16] Z. A. Boeva and V. G. Sergeev, "Polyaniline: Synthesis, properties, and application," *Polym. Sci. Ser. C*, vol. 56, no. 1, pp. 144–153, Sep. 2014.
- [17] "PANi Fiber Actuators, Elisabeth Smela, Professor, Mechanical Engineering, University of Maryland." [Online]. Available: <http://www.smela.umd.edu/polymer-actuators/pani-fiber.html>. [Accessed: 05-Jan-2017].
- [18] H. K. Chaudhari and D. S. Kelkar, "Investigation of Structure and Electrical Conductivity in Doped Polyaniline," *Polym. Int.*, vol. 42, no. 4, pp. 380–384, Apr. 1997.
- [19] G. Momen and M. Farzaneh, "NANOFILLERS - IMPROVING PERFORMANCE AND REDUCING COST." [Online]. Available: http://webcache.googleusercontent.com/search?q=cache:B36zDwjbHP4J:nanopinion.archiv.zsi.at/sites/default/files/observatorynano_briefing_no.21_nanofillers_-_improving_performance_reducing_cost.pdf+&cd=1&hl=en&ct=clnk&gl=pk. [Accessed: 14-Apr-2017].

- [20] H. Mangold and M. Rochnia, "Fumed silica produced by flame hydrolysis, process for its production and its use," 20040253164, 16-Dec-2004.
- [21] Martnez, M. nez-Alanis, Lopez-Urrea, and F. As, "Cement Pastes and Mortars Containing Nitrogen-Doped and Oxygen-Functionalized Multiwalled Carbon Nanotubes," *J. Mater.*, vol. 2016, p. e6209192, Feb. 2016.
- [22] Yumpu.com, "Nanofillers - Improving Performance & Reducing Cost - Nanopinion," yumpu.com. [Online]. Available: <https://www.yumpu.com/en/document/view/52056606/nanofillers-improving-performance-amp-reducing-cost-nanopinion>. [Accessed: 05-Jan-2017].
- [23] J. R. Potts, D. R. Dreyer, C. W. Bielawski, and R. S. Ruoff, "Graphene-based polymer nanocomposites," *Polymer*, vol. 52, no. 1, pp. 5–25, Jan. 2011.
- [24] Z. Wang, J. Luo, and G. Zhao, "Dielectric and microwave attenuation properties of graphene nanoplatelet–epoxy composites," *AIP Adv.*, vol. 4, no. 1, p. 017139, Jan. 2014.
- [25] B. J. Brasjen, H. M. J. M. Wedershoven, A. W. van Cuijk, and A. A. Darhuber, "Dip- and die-coating of hydrophilic squares on flat, hydrophobic substrates," *Chem. Eng. Sci.*, vol. 158, pp. 340–348, Feb. 2017.
- [26] "Dip Coating Technology," Apex Instruments. [Online]. Available: <http://www.apexindia.com/technologies/dip-coating-technology/>. [Accessed: 05-Jan-2017].
- [27] D. Loveday, P. Peterson, and B. Rodgers, "Evaluation of organic coatings with electrochemical impedance spectroscopy. Part 1: Fundamentals of Electrochemical Impedance Spectroscopy," *JCT Coatingstech*, vol. 2, no. 13, pp. 22–27, 2005.
- [28] "Manual for electrochemical corrosion testing and monitoring," vol. 3, 2007.
- [29] "Basics of EIS: Electrochemical Research-Impedance." [Online]. Available: <http://www.gamry.com/application-notes/EIS/basics-of-electrochemical-impedance-spectroscopy/>. [Accessed: 06-Jan-2017].
- [30] Q. Cheng et al., "Corrosion behaviour of Q235B carbon steel in sediment water from crude oil," *Corros. Sci.*, vol. 111, pp. 61–71, Oct. 2016.
- [31] X. Wang and R. E. Melchers, "Corrosion of carbon steel in presence of mixed deposits under stagnant seawater conditions," *J. Loss Prev. Process Ind.*, vol. 45, pp. 29–42, Jan. 2017.
- [32] Y. Jafari, S. M. Ghoreishi, and M. Shabani-Nooshabadi, "Polyaniline/Graphene nanocomposite coatings on copper: Electropolymerization, characterization, and evaluation of corrosion protection performance," *Synth. Met.*, vol. 217, pp. 220–230, Jul. 2016.
- [33] A. Olad, M. Barati, and S. Behboudi, "Preparation of PANI/epoxy/Zn nanocomposite using Zn nanoparticles and epoxy resin as additives and investigation of its corrosion protection behavior on iron," *Prog. Org. Coat.*, vol. 74, no. 1, pp. 221–227, May 2012.
- [34] V. Mišković-Stanković, I. Jevremović, I. Jung, and K. Rhee, "Electrochemical study of corrosion behavior of graphene coatings on copper and aluminum in a chloride solution," *Carbon*, vol. 75, pp. 335–344, Aug. 2014.
- [35] S. Ananda Kumar, K. Shree Meenakshi, T. S. N. Sankaranarayanan, and S. Srikanth, "Corrosion resistant behaviour of PANI–metal bilayer coatings," *Prog. Org. Coat.*, vol. 62, no. 3, pp. 285–292, May 2008.
- [36] L. Y. Xu and Y. F. Cheng, "An experimental investigation of corrosion of X100 pipeline steel under uniaxial elastic stress in a near-neutral pH solution," *Corros. Sci.*, vol. 59, pp. 103–109, Jun. 2012.
- [37] C.-H. Chang et al., "Novel anticorrosion coatings prepared from polyaniline/graphene composites," *Carbon*, vol. 50, no. 14, pp. 5044–5051, Nov. 2012.
- [38] K.-C. Chang et al., "Room-temperature cured hydrophobic epoxy/graphene composites as corrosion inhibitor for cold-rolled steel," *Carbon*, vol. 66, pp. 144–153, Jan. 2014.
- [39] K. S. Aneja, H. L. M. Böhm, A. S. Khanna, and S. Böhm, "Functionalised graphene as a barrier against corrosion," *FlatChem*, vol. 1, pp. 11–19, Jan. 2017.

- [40] R. K. Singh Raman et al., "Protecting copper from electrochemical degradation by graphene coating," *Carbon*, vol. 50, no. 11, pp. 4040–4045, Sep. 2012.
- [41] B. P. Singh, B. K. Jena, S. Bhattacharjee, and L. Besra, "Development of oxidation and corrosion resistance hydrophobic graphene oxide-polymer composite coating on copper," *Surf. Coat. Technol.*, vol. 232, pp. 475–481, Oct. 2013.
- [42] J. Mondal, A. Marques, L. Aarik, J. Kozlova, A. Simões, and V. Sammelselg, "Development of a thin ceramic-graphene nanolaminate coating for corrosion protection of stainless steel," *Corros. Sci.*, vol. 105, pp. 161–169, Apr. 2016.
- [43] J. A. Syed, H. Lu, S. Tang, and X. Meng, "Enhanced corrosion protective PANI-PAA/PEI multilayer composite coatings for 316SS by spin coating technique," *Appl. Surf. Sci.*, vol. 325, pp. 160–169, Jan. 2015.
- [44] G. X. Shen, Y. C. Chen, L. Lin, C. J. Lin, and D. Scantlebury, "Study on a hydrophobic nano-TiO₂ coating and its properties for corrosion protection of metals," *Electrochimica Acta*, vol. 50, no. 25–26, pp. 5083–5089, Sep. 2005.
- [45] M. R. Bagherzadeh and F. Mahdavi, "Preparation of epoxy-clay nanocomposite and investigation on its anti-corrosive behavior in epoxy coating," *Prog. Org. Coat.*, vol. 60, no. 2, pp. 117–120, Sep. 2007.
- [46] M. D. Shittu et al., "Investigation of Corrosion Resistance of Polystyrene as an Inhibitor in Hydrochloric and Tetra-oxo Sulphate VI Acids," *Int. J. Mater. Chem.*, vol. 4, no. 1, pp. 9–13, 2014.
- [47] K. Qi, Y. Sun, H. Duan, and X. Guo, "A corrosion-protective coating based on a solution-processable polymer-grafted graphene oxide nanocomposite," *Corros. Sci.*, vol. 98, pp. 500–506, Sep. 2015.
- [48] D. Loveday, P. David, and B. Rodgers, "Evaluation of organic coatings with electrochemical impedance spectroscopy - Part 2: Application of EIS to coatings," *JCT Coatingstech*, vol. 2, no. 13, pp. 22–27, 2005.
- [49] Y.-H. Yu, Y.-Y. Lin, C.-H. Lin, C.-C. Chan, and Y.-C. Huang, "High-performance polystyrene/graphene-based nanocomposites with excellent anti-corrosion properties," *Polym. Chem.*, vol. 5, no. 2, pp. 535–550, 2014.
- [50] M. Kendig and J. Scully, "Basic Aspects of Electrochemical Impedance Application for the Life Prediction of Organic Coatings on Metals," *CORROSION*, vol. 46, no. 1, pp. 22–29, Jan. 1990.
- [51] F. Deflorian, L. Fedrizzi, S. Rossi, and P. L. Bonora, "Organic coating capacitance measurement by EIS : ideal and actual trends," *Electrochimica Acta*, vol. 44, no. 24, pp. 4243–4249, 1999.
- [52] A. Mostafaei and F. Nasirpouri, "Epoxy/polyaniline-ZnO nanorods hybrid nanocomposite coatings: Synthesis, characterization and corrosion protection performance of conducting paints," *Prog. Org. Coat.*, vol. 77, no. 1, pp. 146–159, Jan. 2014.
- [53] W.-K. Lu, R. L. Elsenbaumer, and B. Wessling, "Corrosion protection of mild steel by coatings containing polyaniline," *Synth. Met.*, vol. 71, no. 1, pp. 2163–2166, Apr. 1995.
- [54] T. ul H. Zia, A. N. Khan, M. Hussain, I. Hassan, and I. H. Gul, "Enhancing dielectric and mechanical behaviors of hybrid polymer nanocomposites based on polystyrene, polyaniline and carbon nanotubes coated with polyaniline," *Chin. J. Polym. Sci.*, vol. 34, no. 12, pp. 1500–1509, Dec. 2016.
- [55] N. T. Kirkland, T. Schiller, N. Medhekar, and N. Birbilis, "Exploring graphene as a corrosion protection barrier," *Corros. Sci.*, vol. 56, pp. 1–4, Mar. 2012.
- [56] T. Monetta, A. Acquesta, and F. Bellucci, "Graphene/Epoxy Coating as Multifunctional Material for Aircraft Structures," *Aerospace*, vol. 2, no. 3, pp. 423–434, Jun. 2015.